

27
13/84
AB

I-12641 ①

DR-2015-X

UCRL-53445

Characteristics of the Eleana Formation, Nevada Test Site

J. J. Sweeney

November 10, 1983



MASTER

DISTRIBUTION OF THIS DOCUMENT IS UNLIMITED

DISCLAIMER

This report was prepared as an account of work sponsored by an agency of the United States Government. Neither the United States Government nor any agency thereof, nor any of their employees, makes any warranty, express or implied, or assumes any legal liability or responsibility for the accuracy, completeness, or usefulness of any information, apparatus, product, or process disclosed, or represents that its use would not infringe privately owned rights. Reference herein to any specific commercial product, process, or service by trade name, trademark, manufacturer, or otherwise does not necessarily constitute or imply its endorsement, recommendation, or favoring by the United States Government or any agency thereof. The views and opinions of authors expressed herein do not necessarily state or reflect those of the United States Government or any agency thereof.

DISCLAIMER

Portions of this document may be illegible in electronic image products. Images are produced from the best available original document.

DISCLAIMER

This document was prepared as an account of work sponsored by an agency of the United States Government. Neither the United States Government nor the University of California nor any of their employees, makes any warranty, express or implied, or assumes any legal liability or responsibility for the accuracy, completeness, or usefulness of any information, apparatus, product, or process disclosed, or represents that its use would not infringe privately owned rights. Reference herein to any specific commercial products, process, or service by trade name, trademark, manufacturer, or otherwise, does not necessarily constitute or imply its endorsement, recommendation, or favoring by the United States Government or the University of California. The views and opinions of authors expressed herein do not necessarily state or reflect those of the United States Government thereof, and shall not be used for advertising or product endorsement purposes.

UCRL--53445

DE84 004138

Characteristics of the Eleana Formation, Nevada Test Site

J. J. Sweeney

Manuscript date: November 10, 1983

LAWRENCE LIVERMORE NATIONAL LABORATORY 
University of California • Livermore, California • 94550

Available from: National Technical Information Service • U.S. Department of Commerce
5285 Port Royal Road • Springfield, VA 22161 • \$10.00 per copy • (Microfiche \$4.50)

NOTICE

PORTIONS OF THIS REPORT ARE ILLEGIBLE.

**It has been reproduced from the best
available copy to permit the broadest
possible availability.**

jb
DISTRIBUTION OF THIS DOCUMENT IS UNRESTRICTED

TABLE OF CONTENTS

Abstract	1
I. Introduction	2
II. General Geologic Setting, Stratigraphy, and Previous Studies	4
Summary	10
III. Composition of Eleana Formation Rocks	10
Summary	14
IV. Physical Properties	14
Density, Porosity, and Water Content	14
Seismic Velocity and Mechanical Properties	18
Electrical, Thermal, and Hydrologic Properties	27
Summary	29
V. Structural Setting of the Eleana Formation	29
Characteristics of Thrust Faulting	30
Structural Setting of the Western Side of Yucca Flat and Areas to the North and South	37
Assessment of Sites Appropriate for Underground Testing in Argillite	42
The Syncline Ridge Area	43
The Mid Valley Area	43
The Calico Hills Area	43
The Yucca Flat Area	43
Summary	46
VI. Conclusions and Recommendations	46
Acknowledgment	47

CHARACTERISTICS OF THE ELEANA FORMATION, NEVADA TEST SITE

ABSTRACT

Data concerning the physical properties and the surface and subsurface occurrence of the Eleana Formation are compiled here, to assess argillite as a possible testing medium. This study focuses on the upper part of the formation, since the data are available and suitable units are also available for subsurface testing. The data are sufficient for a good characterization of physical properties, but the assessment of structural complexity is more difficult. Eventually, in an exploration phase, the physical properties and lithologic variations at a particular site can be well characterized with geophysical logging. A preliminary examination of published maps and cross sections leads to the conclusion that the structure of Paleozoic rocks at the NTS (particularly in the Yucca Flat area), is not well known. At this time, therefore, only a speculative assessment of the subsurface extent of Eleana Formation argillite can be made.

I. INTRODUCTION

The Eleana Formation is of middle-to-upper Paleozoic age, and is one of the more widely-exposed pre-Mesozoic rock units at the Nevada Test Site (NTS). This report assembles existing data from a variety of sources for use in assessing the Eleana Formation's potential as a nuclear testing medium. At present, the properties of Paleozoic rocks are not routinely determined at the NTS.¹ Consequently, few data are available from the Test Program archives. However, the Yacht (Plowshare) program of the early 1970's, and the United States Geological Survey's (USGS's) Waste Management Program of the late 1970's, acquired a large quantity of data on the upper part of the Eleana Formation. Sections III and IV of this report are a compendium of the data from these two major programs, and from other sources.

Areas where Eleana Formation rocks are exposed at the NTS² are shown in Fig. 1. Other areas, where the Eleana and equivalent formations are exposed near the NTS, have also been described.^{3,4} The most prominent of these exposures are in the Belted Range in Nellis AFB,⁵ and in the Calico Hills,⁶ C. P. Hills,⁷ Mine Mountain,^{8,9} Eleana Range,⁹ and Quartzite Ridge¹⁰ areas within the NTS. The Eleana Formation has been discovered in the subsurface beneath Yucca Flat, and beneath alluvium east of Eleana Ridge by drilling.^{11,12} It is also inferred (by mapping) as being buried beneath the alluvium west of Mine Mountain.⁸ Based on subsurface geology and topographic slope considerations, a previous investigation¹³ identified areas where drill holes and horizontal tunnel sites would possibly encounter Eleana Formation rocks.

The structural setting of the Eleana Formation in southern Nevada is complex. All of the Paleozoic rocks have been significantly deformed by post-Paleozoic thrust faults, folds, and lateral faults, and by Mesozoic and Cenozoic igneous intrusions and extensional tectonics.² In the Eleana Formation, three important manifestations of these deformations are:

- zones of weakness, caused by shearing;
- changes in layering orientation, due to folding and thrusting;

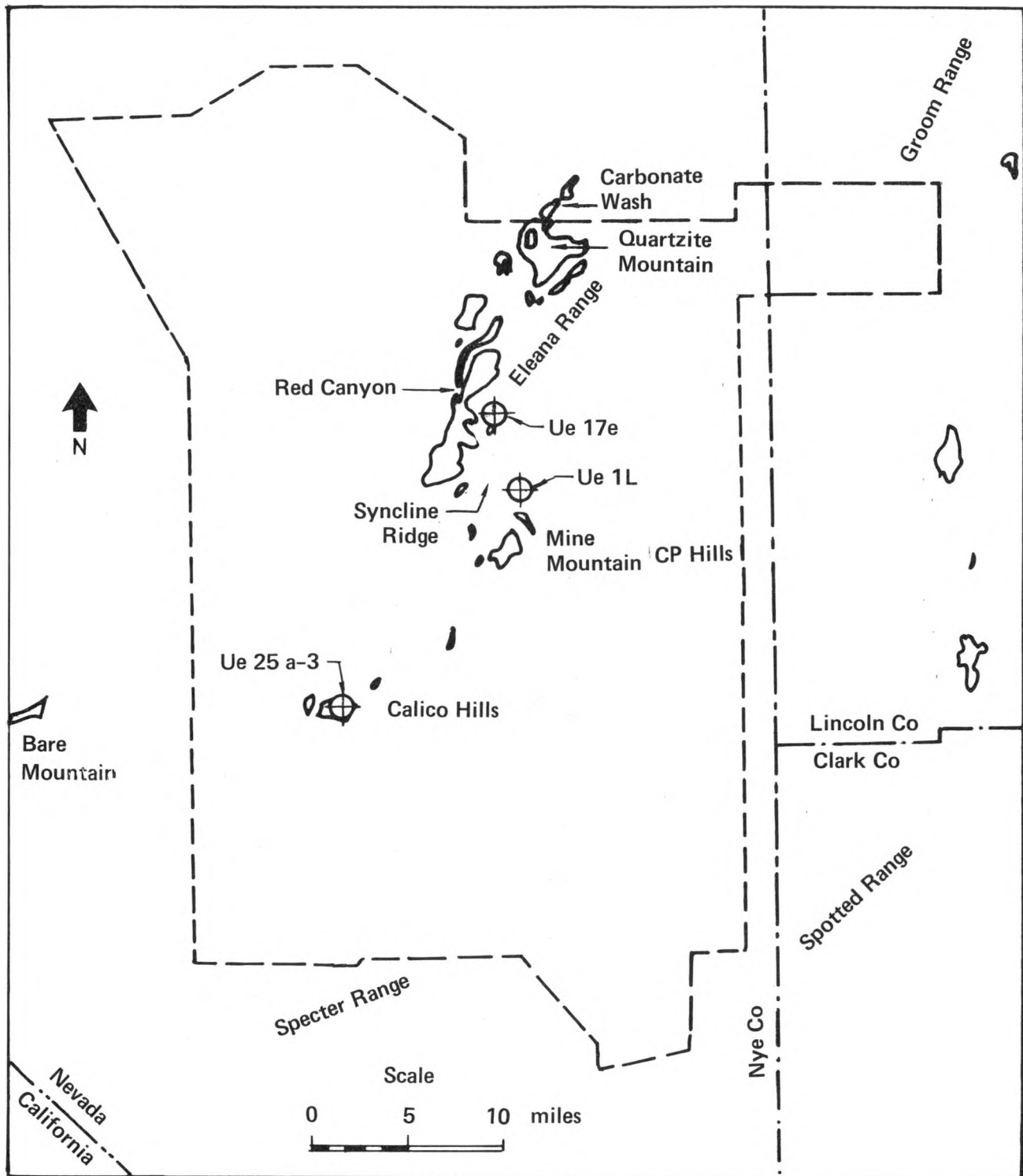


Fig. 1. The distribution of exposed Mississippian rocks in the NTS area (modified from Sinnock²), including the locations of deep holes drilled into the Eleana Formation.

- the repetition of lithologic units in boreholes, due to thrust faulting.

A brief general tutorial on fold and thrust deformation features is given in Section V, along with a detailed discussion of these features as applied to the conditions expected in the Eleana Formation.

In an early study,¹⁴ the Eleana Formation was subdivided into ten stratigraphic units, labelled A (the oldest) through J (the youngest). Descriptions of these subunits^{12,13} indicate that argillite, quartzite, and carbonate are present in various proportions. Unit J, the uppermost unit, contains a section (up to 700 m thick) of massive argillite, with minor occurrences of quartzite and rare carbonate. Unit J is also the most easily accessible to drilling in the Yucca Flat and Mine Mountain areas. For these reasons it was chosen as the primary subject for study by the Yacht and Waste Isolation Projects. Therefore, the bulk of the available data pertains to that unit.

The units below J are not being considered in this preliminary study because of the nature of their lithology and their relatively inaccessible location with regard to drilling (900 m in depth). Also, since only small amounts of physical property data are available on units A through I, this study will focus on the argillite of unit J.

II. GENERAL GEOLOGIC SETTING, STRATIGRAPHY, AND PREVIOUS STUDIES

The surface areal occurrence of the Eleana Formation at the NTS was just mentioned, and the reader is again referred to Fig. 1. The Eleana Formation was named by Johnson and Hibbard (1957).¹⁵ It ranges in age from late Devonian to late Mississippian,^{13,14,16} probably in a continuous section. However, because of its structural complexity and discontinuous outcrop, the Eleana Formation is known only through partial sections. In the Carbonate Wash area, the unit is about 2350 m thick.^{5,13} Further south, in the Syncline Ridge area, it might possibly be as thick as 3000 to 4000 m.¹² The Eleana Formation lies unconformably on Devonian dolomite and limestone, and is overlain by the

Tippipah limestone,^{2,13} of Pennsylvanian/Permian age. The contact with the Tippipah is probably a disconformity.¹³

Lithologies present in the Eleana Formation reflect conditions of siliceous sediment deposition, originally in an rapidly-subsiding basin, with periods of quiescence marked by limestone deposition.¹² The depositional setting was in a north-northeast trending trough extending from California to Idaho, east of a highland built up during the emplacement of the Roberts Mountain allochthon (during the late-Devonian early-Mississippian Antler Orogeny). A map of late-Mississippian lithofacies¹⁶ (Fig. 2) shows the location of the flysch (mudstone, sandstone, siltstone, and conglomerate) of the Eleana and equivalent formations, with respect to the Antler Orogenic Highland. Near the end of the Antler Orogeny, deep weathering of the lower highlands resulted in the deposition of predominantly clay minerals in the upper part of the Eleana.¹²

The Eleana Formation was divided into ten subunits by Poole, et al.,¹⁴ and labeled A (lowest) through J (highest). In general, the trend is for coarser, more siliceous sediments to be at the bottom with finer sediments occurring at the top. Units A, C, D, F, G, and I contain considerable amounts of limestone, quartzite, and conglomerate, while units B, E, H, and J are predominantly argillite*.^{5,12-14} Figure 3 describes the four upper units, showing their relation to one another and to the Tippipah limestone. Note that Hodson and Hoover¹⁷ divided unit J into a lower unit (about 300 m thick), an argillite unit (about 700 m thick), and an upper quartzite unit (about 100 m thick). The middle argillite unit was targeted for exploration by both the Yacht and Waste Isolation programs (though it was not subdivided as such in the Yacht project).

Hoover and Morrison¹² give extensive descriptions (for mapping purposes) of units G through J and the subunits of J, which are only summarized in Fig. 3. The middle argillite unit of J contains massive

*"Argillite" refers to a rock derived from mudstone (claystone or siltstone) or shale, which is more indurated (cemented) and less clearly laminated or fissile than shale. Shale generally splits along thin partings parallel to its layering.¹⁸

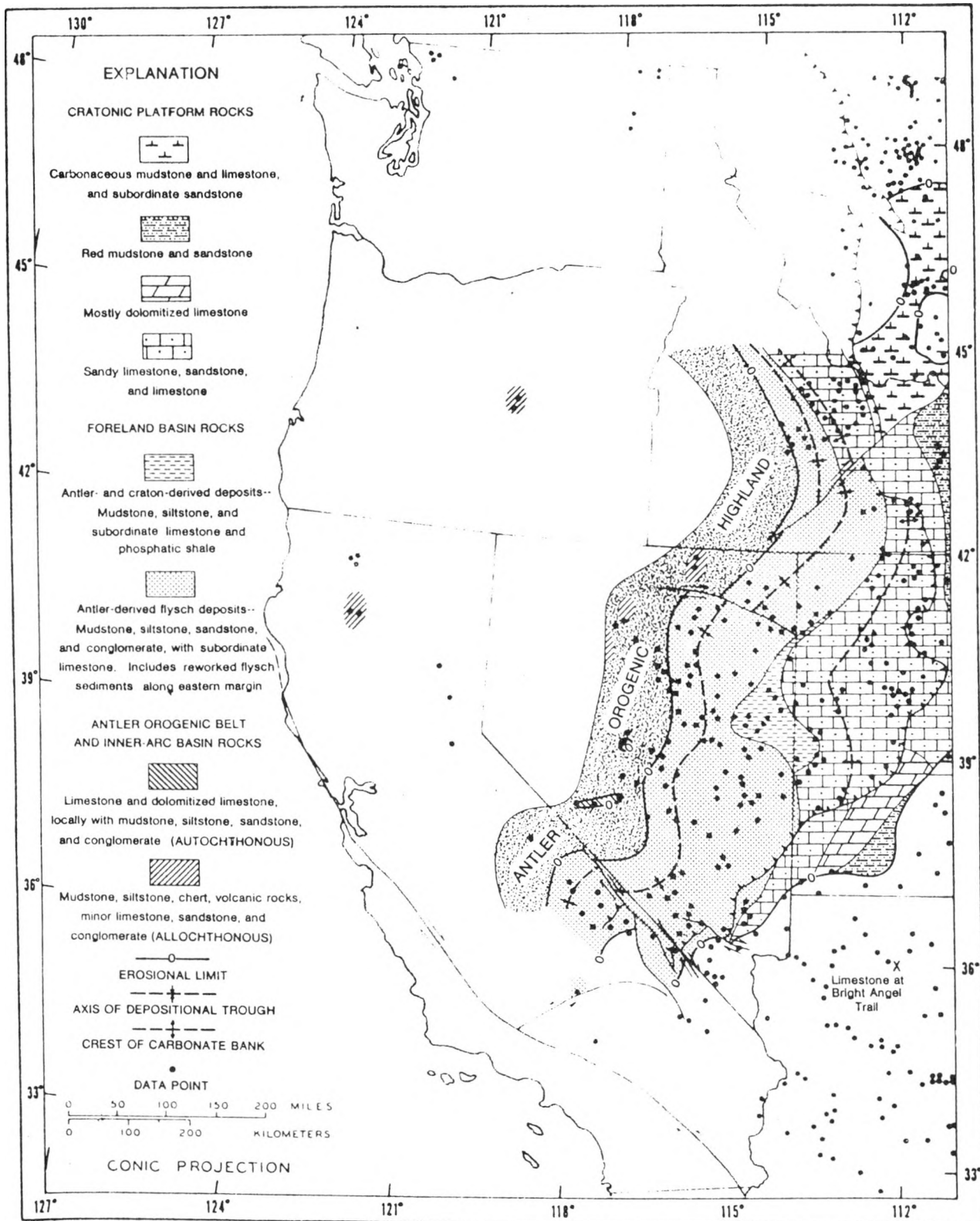


Fig. 2. Lithofacies map (partly restored) of the Upper Mississippian (Middle and Upper Meramecian and Chesterian) rocks. (From Poole and Sandberg.¹⁶)

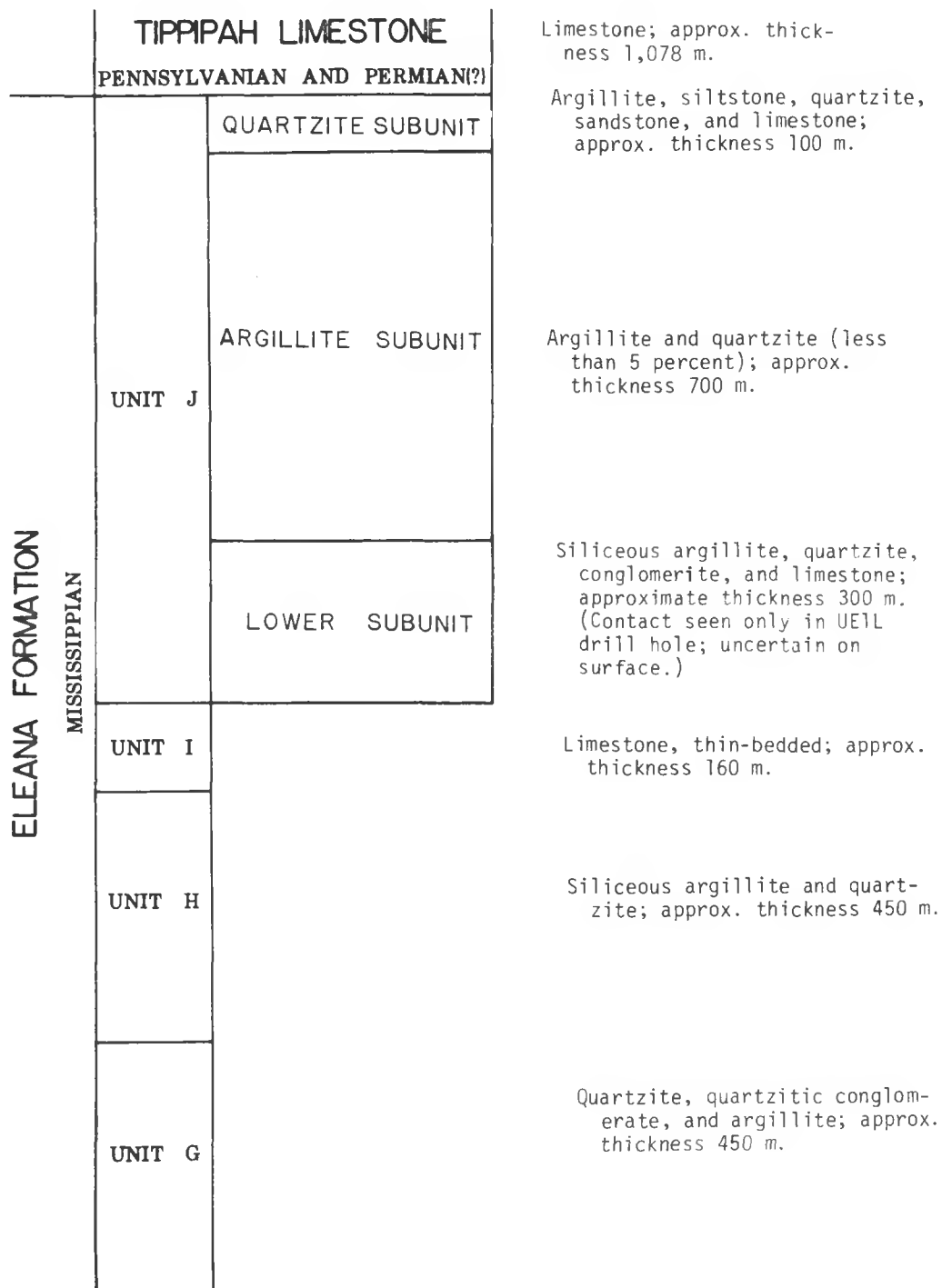


Fig. 3. The pre-Tertiary stratigraphic units of the Syncline Ridge area.
(From Hodson and Hoover.¹⁷)

argillite with a quartzite bed near the middle, and at least three other intervals near the base. The total amount of quartzite in the subunit is less than 5 percent, with no limestone. Both the upper and lower subunits of J contain numerous siltstone, quartzite, and limestone beds of up to several meters in thickness. Further descriptions of the composition and physical properties of unit J rocks are given in Sections III and IV.

As mentioned earlier, much of our knowledge about the Eleana Formation comes from the documentation associated with two major programs carried out within the past 12 years. The Yacht program, part of Plowshare, was a project designed to examine the feasibility of using sequentially-detonated nuclear devices to enhance the permeability of shale for eventual gas recovery. An exploratory hole 1627 m (5339 ft) in depth, UelL, was drilled just east of Syncline Ridge through 80 m of alluvium into unit J. Before bottoming in the lower quartzite subunit of J, the hole encountered numerous shear zones and probably a thrust fault that caused a major repetition in the section.¹² Core samples from UelL were analysed by Terra Tek¹⁹ for physical properties. Chemical and x-ray analyses were also performed.^{20,21} In an attempt to learn more about the local structure, a Vibroseis^(R) seismic survey was done: the results were inconclusive, due to poor data.²² The USGS carried out electrical sounding surveys,^{23,24} which found that the apparent resistivities of argillite were an order of magnitude lower than for limestone or quartzite. These surveys also predicted a depth to the bottom of argillite of 4800 feet (1463 m) +20%. Other details about the structure beneath Yucca Flat to the east of UelL were available from previously drilled holes^{25,26} that had encountered the Eleana Formation.

One result of the Yacht project was a set of SOC code calculations completed by M. D. Denny,²⁷ which used data from the Terra Tek report, LLL tests, and assumptions based on experience with previous tests in the Lewis and Wagon Wheel shales. The results of these calculations are reproduced in Appendix A.

A study predicting the ground motion resulting from a proposed Yacht event was done by Bernreuter and Jackson.²⁸ The calculations were done for a 6000 ft (1828.8 m) depth of burial, and a 100 kt yield. Much greater ground motion than experienced in the past was predicted, with

impact accelerations of from 10 to 30 g's at site ground zero and peak g levels in the frequency range of from 10 to 20 Hz. Funding was terminated before any detonations were done in the Yacht hole.

In the late 1970's, a series of investigations were carried out to determine the suitability of the Eleana Formation as a nuclear waste repository medium. The sites selected for study were the Syncline Ridge area between Mine Mountain and the Eleana Range, and the Calico Hills. The prime investigator was the USGS, with a heater experiment done by Sandia. A series of exploratory holes were drilled to better define the structure: Uel6b, c, d and Uel7a, b, c, d were the principal holes in this series. A major effort was expended on Uel7e,¹⁷ 914.4 m (3000 ft) deep, located at the northwest corner of Syncline Ridge, and on Ue25a-3,²⁹ 771.2 m (2530 ft) deep, located in the Calico Hills area. The locations of Uel7e, Ue25a-3, and UelL are shown in Fig. 1. Both Uel7e and Ue25a-3 encountered unit J of the Eleana Formation: the former went through the upper two subunits of J, and the latter went through the lower two subunits of J and the upper part of unit I. Extensive core was recovered, and detailed fracture analyses and physical property tests were done. These tests have provided much of the data used in Section IV of this report. The deeper units in Ue25a-3 were interpreted as having been thermally altered by an igneous intrusion at depth. Sets of geophysical logs run in both holes included resistivity, 3-D velocity, caliper, and density. Hydrologic tests were carried out in Uel7a,³⁰ Uel6d, and Uel6f.³¹ Summaries of the geology and lithology in the holes drilled for the waste isolation program are recorded in a series of reports.^{12,17,32} Resistivity soundings³³ and other geophysical surveys³⁴ were carried out to refine knowledge of the structure of the Syncline Ridge area. The results of a heater experiment in shallow holes near Uel7e were reported by Sandia.³⁵

Additional information concerning the locations of holes in Yucca Flat that have encountered Eleana Formation rocks is provided by McArthur¹¹ and Fernald, et al.³⁶ A limited amount of physical property data on the Eleana is given in McKague.¹ Appendix B lists the drill holes into the Eleana Formation that were studied for this report.

Summary

Results from the Yacht (Ue1L) and waste isolation (Ue17e) boreholes provide a good data set for looking at variations of properties over a distance of about 5 km. The Calico Hills hole (Ue25a-3) is more distant (approximately 22 km from Ue1L), but the formation there has been partially thermally altered. However, fracture and mechanical property data comparisons between and among the three holes still provide a useful means for assessing the areal continuity of parameters (see Section IV).

III. COMPOSITION OF ELEANA FORMATION ROCKS

Shale and argillite are clastic rocks containing a large fraction of sheet silicate minerals, such as mica and clay. Argillite generally refers to a rock which is more indurated than shale and has a lesser tendency to be fissile. Hoover and Morrison,¹² in mapping unit J of the Eleana Formation, divided the middle argillite unit into three subsets. They used the term "siliceous argillite" for argillite containing more than 90% quartz. This part of the formation has a resistivity of greater than 50 ohm-m. Argillite with less than 90% quartz and a resistivity of less than 30 ohm-m was referred to as "argillaceous argillite." This latter rock was further subdivided into a high-quartz argillite (HQA) containing 25 to 45% quartz, and a low-quartz argillite (LQA) with less than 25% quartz. These subdivisions (illustrated in Fig. 4) have important implications for physical properties, and are discussed further in Section IV.

Siliceous argillite comprises mainly the upper quartzite zone (100 m) of Unit J and parts of the lower zone (300 m). Most of unit J consists of argillaceous argillite (700 m) with layers of HQA and LQA alternating in an unpredictable manner. Hoover and Morrison¹² were unable to conclude whether these HQA-LQA alternations were tectonically or depositionally controlled.

HQA and LQA can be distinguished in a drill hole from the API neutron log. HQA is generally marked by an API neutron index that is greater than 700. LQA has an API neutron index of less than 600. The P-wave

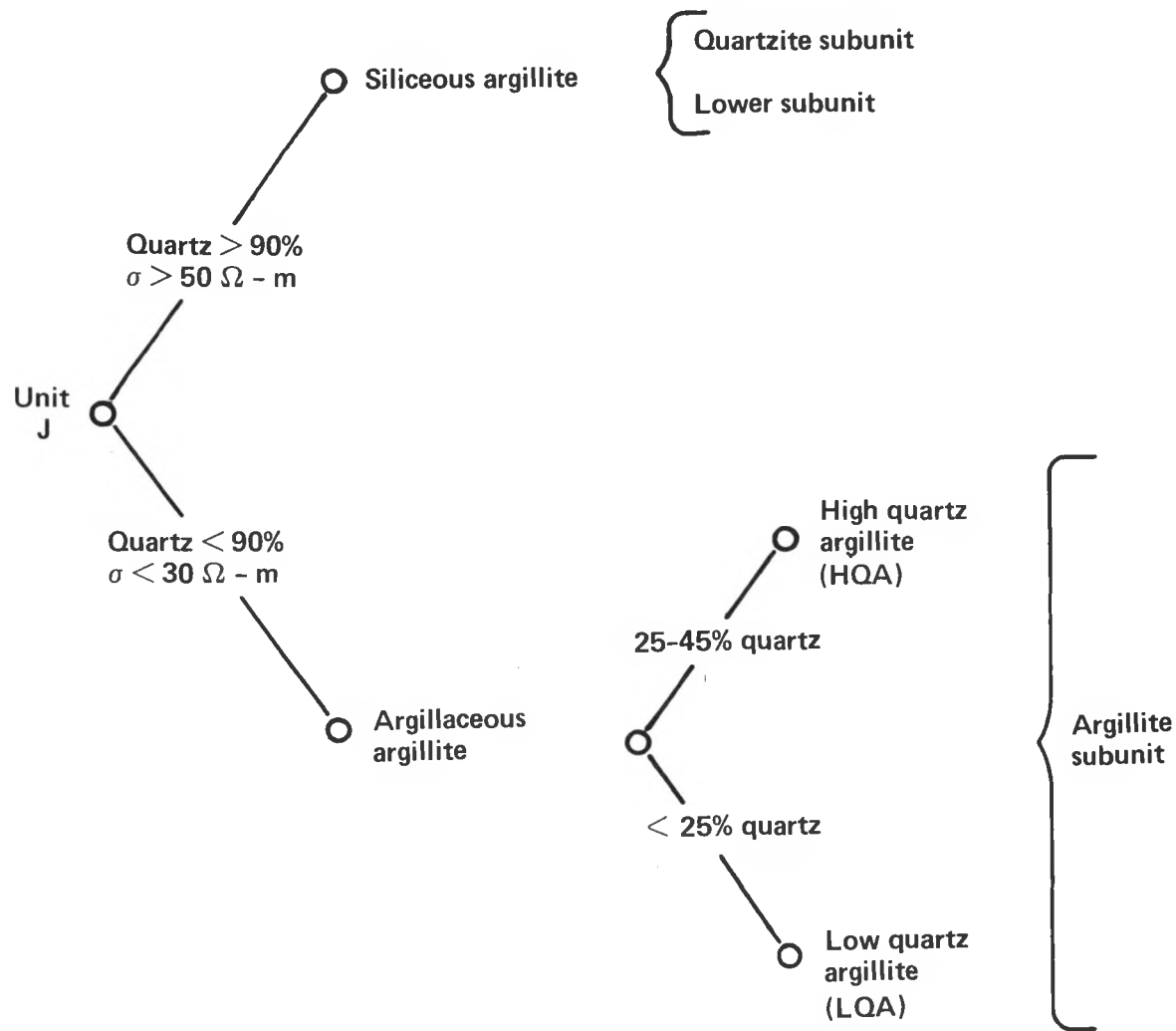


Fig. 4. Subdivisions of the argillite subunit (σ refers to the resistivity of the rock mass).

velocity is also a function of quartz content. Correlating the 3-D velocity logs with core samples¹² gives the following values:

<u>P Velocity (km/s)</u>	<u>Percentage of LQA Layers</u>
3.5 - 4.0	< 10%
3.5 - 3.6	10 - 30%
3.0 - 3.5	> 30%

Except for the difference in quartz content,¹² the LQA and HQA zones are mineralogically similar. An examination of the chemical and mineralogical data for various parts of the Eleana Formation should give a good estimate of compositional variations in the non-quartz fraction.

Argillite samples from the argillite subunit of Unit J in the Calico Hills were reported²⁹ as containing 30% to 40% quartz (making it HQA), with the rest of the minerals being mixed layers of illite and illite-montmorillonite. Other minerals that are present in lesser amounts are feldspar, calcite, chlorite, and siderite. Typical fracture-filling minerals are kaolinite-dickite, nacrite, and chlorite. A sample from UelL²¹ (LQA) gave a similar analysis. The principal minerals were quartz (20%), 20% layered illite-montmorillonite (with an illite content of 80%), chlorite (20%), kaolinite (10%), illite and mica (10%). Of 60 argillite samples from the Syncline Ridge area,¹² all contained quartz, illite, and montmorillonite, 72% contained pyrophyllite, and 13% contained calcite. The percent concentrations of individual minerals in the samples were not given. The carbonate content in the argillite subunit is relatively low. Hill²⁰ reported weight percentages of CO₂ in UelL of 0.25 to 2.83 in the argillite unit (depths < 1300 m), and a weight percentage of CO₂ ranging from 0.89 to 10.83 in the lower unit (depths > 1560 m), which is known to contain limestone layers.³⁷ Samples analyzed by TerraTek¹⁹ from the Yacht hole contained 3% carbonate by volume.

Chemical analyses from the Yacht hole²⁰ and the Syncline Ridge study¹² are compared in Table 1. These are similar to results obtained by Turner.³⁸ The composition of the samples is typical of most shales, high in silica and alumina, and low in carbonate. The two data sets differ by only a few percent, indicating that (in the southwestern Yucca

Flat area) the argillite unit of J is compositionally quite uniform. Although detailed data are not available from published sources, the Calico Hills argillite²⁹ probably differs very little in composition from that of Yucca Flat. While detailed compositional data are not available for units other than unit J, the consistency of the source area and depositional environment of the Eleana Formation throughout Mississippian time argues for a relatively uniform composition throughout (except for quartz and carbonate). The data on free and bound water content and saturation are discussed, along with porosity and permeability data, in Section IV.

Table 1. Chemical analyses of the argillite from unit J.

Constituent	Set A ^a		Set B ^b	
	Mean	Range	Mean	Range
SiO ₂	58.3	53.7 - 65.4	55.1	52.7 - 58.3
Al ₂ O ₃	20.2	16.4 - 27.1	23.4	20.0 - 25.7
Fe ₂ O ₃	--	--	6.9	5.7 - 7.8
Fe ₂ + FeO	5.7	2.4 - 9.1	--	--
CaO	0.7	0.28 - 1.16	0.9	0.7 - 1.4
CO ₂	--	--	1.5	0.3 - 2.8
H ₂ O + CO ₂	8.5	7.1 - 10.4	--	--
H ₂ O ⁺	6.5	5.4 - 7.4	--	--
H ₂ O ⁻	--	--	0.9	0.7 - 1.1

^a Sample set A represents data averaged from eight samples,¹² which are presumed to be percent by weight, although whether the data were weight or volume fraction was not specified.

^b Sample set B is weight-fraction data, as determined by Hill²⁰ on four samples from depths of less than 1290 m in the Yacht hole.

Summary

The siliceous and argillaceous argillite compositions in the Eleana Formation differ primarily in their quartz content. The composition of the non-quartz fraction is quite uniform, consisting primarily of illite and chlorite, with lesser concentrations of montmorillonite and kaolinite. The carbonate content is less than 5% in the massive argillaceous argillite of unit J, which is about 700 m thick. Limestone layers are known to occur in the upper and lower portions of unit J and are much more prevalent in units A, C, D, F, G, and I. The other argillaceous units of the Eleana Formation (B, E, and H) are probably similar in gross composition to unit J.

IV. PHYSICAL PROPERTIES

Density, Porosity, and Water Content

The various types of measurements used to determine density, porosity, and water content are described by McKague.¹ Once again, the available data for the Eleana Formation come mainly from the Yacht program, and the USGS's Waste Isolation program. The method of measurement is often not specified. Many of the USGS's measurements were done on core samples by Holmes and Narver, Inc., located at Mercury, Nevada.^{29,32} Table 2 lists the results of measurements on core samples from UeLL (Yacht) that were done by Turner,³⁹ Terra Tek,¹⁹ and LLNL.²⁷ The physical property terms are listed as they were used in the various reports. Some properties may be equivalent; e.g. the calculated gas porosity (given as a fraction) and the calculated porosity (given as a percentage). Because the true nature of each measurement has not been determined for this report, the data are given as they are listed in the references. At the bottom of Table 2, the bulk density data are listed as determined from borehole logs for three drill holes. These data are about 5% less than the bulk density as measured on core samples. Hoover and Morrison¹² attribute this to the fractured nature of the argillite in situ.

Table 2. Mean values for the density in g/cm³, porosity, and water content of the Eleana shale's unit J argillite. The range is in parentheses: n is the number of samples.

Property	Turner ³⁹ UelL n = 5	Terra Tek ¹⁹ n = 5 [n = 3]	Syncline Ridge ¹² n = 33	Calico Hills ²⁹ (Ue25a-3) n = 11	McKague ¹ (Uel7e)
Bulk Density:					
Wet ^a	2.641 (2.628-2.655)	2.64 (2.58-2.66)	2.62 (2.51-2.75)	2.59 (2.47-2.67)	2.62 --
Dry	2.614 (2.609-2.618)	-- --	-- --	2.52 (2.34-2.59)	-- --
Grain Density	2.847 (2.820-2.868)	2.73 [2.72-2.75]	2.78 (2.68-2.95)	2.75 (2.70-2.88)	2.79
Gas Porosity					
Calculated	0.0817 (0.0721-0.0879)	-- --	-- --	-- --	-- --
Measured	0.0547 (0.0473-0.0612)	-- --	-- --	-- --	-- --
Porosity					
Calculated	-- --	-- --	-- --	8.55% (4.9-13.3%)	-- --
Measured	-- --	-- --	8.15% (2.7-13.5%)	10.22% (3.6-20.9%)	8.9% (Vol.) --
Saturation	-- --	-- --	-- --	82.6% (36-100%)	8.6% (Calc.) --
Water Content	-- --	-- --	3.60% (0.36-4.7%)	-- --	2.78% (wt.) --
Weight fraction					
H ₂ O	1.40 (1.01-1.60)	-- --	-- --	-- --	-- --

^a Also referred to as the "natural state" density; ¹² measured on recovered core.

Bulk density from borehole logs: UelL n = 180 Uel6d n = 136 Uel7e n = 276
 2.36 2.47 2.51
 (2.02-2.57) (2.02-2.66) (1.85-2.73)

The natural-state (wet) bulk density of 2.62 g/cm^3 given by McKague seems to be representative of values for unit J in the Syncline Ridge area. Samples from the Yacht hole (UeLL) came from greater depths and the higher bulk density in those samples may reflect greater compaction. Samples from the Calico Hills (Ue25a-3) hole have generally lower bulk density values and slightly higher porosity. This may be due to fracturing related to an igneous intrusion at depth and an accompanying hydrothermal alteration. No attempt was made in the Hoover and Morrison¹² report to correlate bulk density, grain density, or porosity data with the HQA and LQA zones.

The typical variation of density with depth can be seen in Fig. 5, a log of density and corrected density for the lower part of unit J, at a depth of from 4300 to 4900 ft (1310.6 to 1493.4 m) in UeLL. The boundary between the argillaceous argillite unit and the lower subunit is marked at 4630 ft (1411.2 m) by an abrupt increase in the average density, presumably due to an increase of quartz content in the siliceous argillite of the lower subunit. The cause of the rapid excursions in the density log of the argillite from 4300 to 4600 ft (1310.6 to 1402.0 m) in depth is unknown, but they are probably due to changes in fracture frequency, because bulk density measurements made on core samples in this range do not show a wide variation.

The data from the Hoover and Morrison report¹² are the most representative of the properties to be expected from the Mine Mountain/Yucca Flat/Eleana Ridge area. Representative values are:

Natural state bulk density	2.62 g/cm^3
Grain density	2.78 g/cm^3
Porosity (volume)	5 - 8%
Water content (weight)	3.6%
Saturation	86 - 100%

An initial natural-state bulk density of 2.66 g/cm^3 and a water content of 10% by weight was used by Denny in the SOC code calculations (Appendix A).

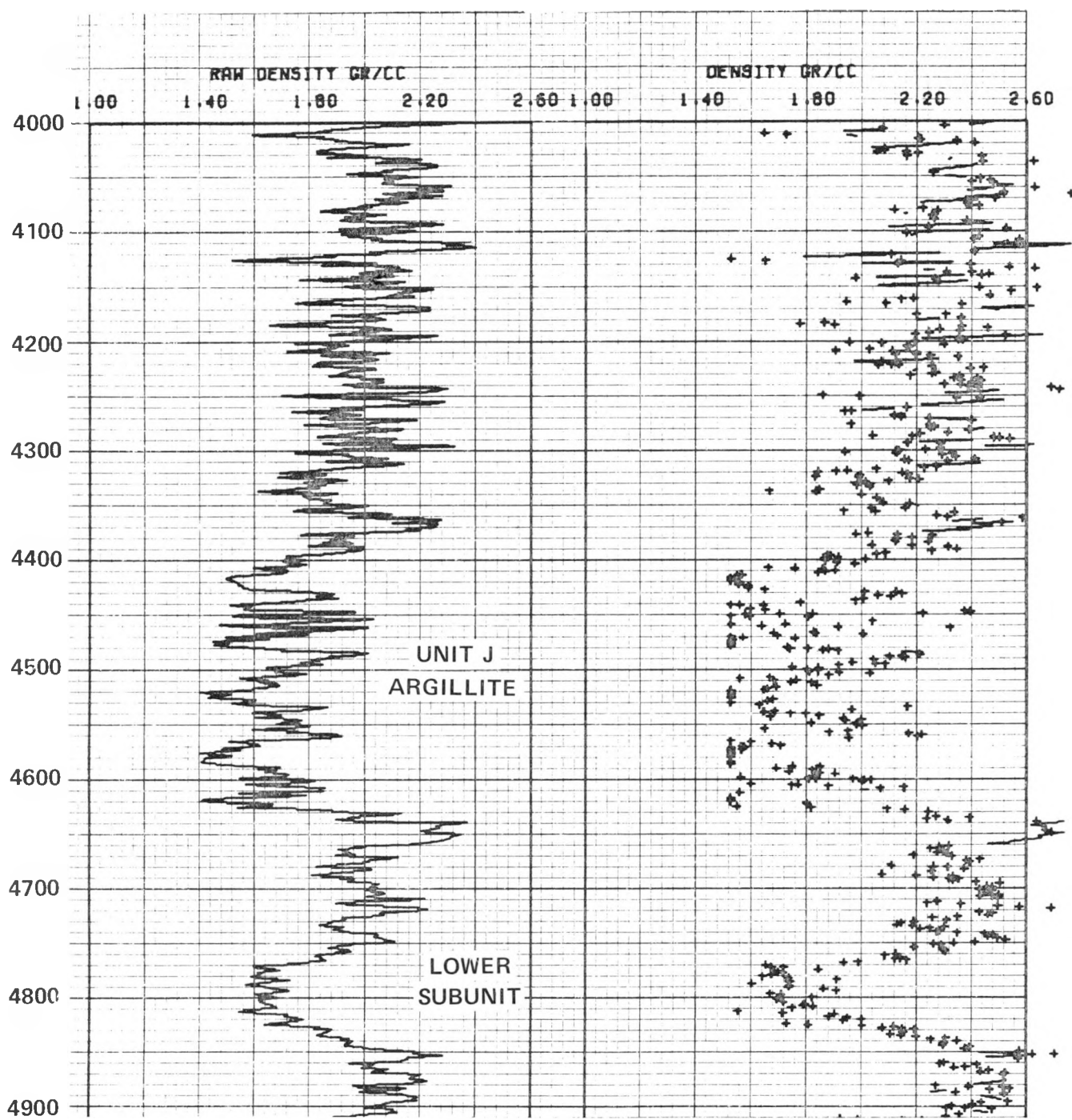


Fig. 5. The calculated density, and density-log data from Uell.

Seismic Velocity and Mechanical Properties

Sonic velocity logs were obtained from many of the drill holes used in the Yacht and Waste Isolation projects. The author knows of no velocity data taken on core. Dry hole acoustic logs (DHAL), 3-D logs, and Vibroseis^(R) logs have been used. Mechanical properties, such as Poisson's ratio and Young's modulus can be calculated from compressional (V_p) and shear wave (V_s) velocity and density data, or measured in the laboratory by testing core samples. Compression, extension, and uniaxial-strain tests were carried out on argillite cores of units J and I, from the 4209 to 4230 ft (1282.9 to 1289.3 m) and the 5144 to 5155 ft (1567.9 to 1571.2 m) depths, respectively, of UeL¹⁹. Core samples from holes Ue17e and Ue25a-3 were tested by Holmes and Narver,^{12,29} resulting in determinations of unconfined compressive strength, Young's modulus, and Poisson's ratio.

Figure 6 compares logs of 3-D velocity (V_p and V_s) from the 4300 to 4850 ft (1310.6 to 1478.2 m) level in UeL to the caliper and density logs for the same interval. The boundary between the argillaceous argillite of unit J and the siliceous argillite/quartzite/limestone of the lower subunit of J is marked by sharp changes in average values on each of the logs. As mentioned in Section III, Hoover and Morrison¹² noted a correlation between V_p and the argillite's quartz content: lower-velocities correlate with a lesser quartz content. Hoover and Morrison¹² also report that V_p (from the 3-D, or the DHAL) is most useful for identifying zones where less than 10% of the layers are LQA, because this diagnostic is more definitive than the neutron log. In general, the Vibroseis^(R) velocities are lower than those obtained from the 3-D or DHAL¹² logs.

The velocity logs (travel-time data) have not been reduced to give velocities for drill holes other than for UeL and Ue25a-3, and these data are only for the lower portion of each hole. From Fig. 6 (UeL) it can be seen that the average V_p is about 3.2 km/s in the argillite, with a range of from 2.0 to 4.5 km/s. In the argillite, the average V_s is about 1.7 km/s, with a range of from 1.0 to 2.3 km/s. Both V_p and V_s are higher in the lower subunit of Unit J (and in unit I below it) because of the presence of quartzite, limestone, and siliceous argillite

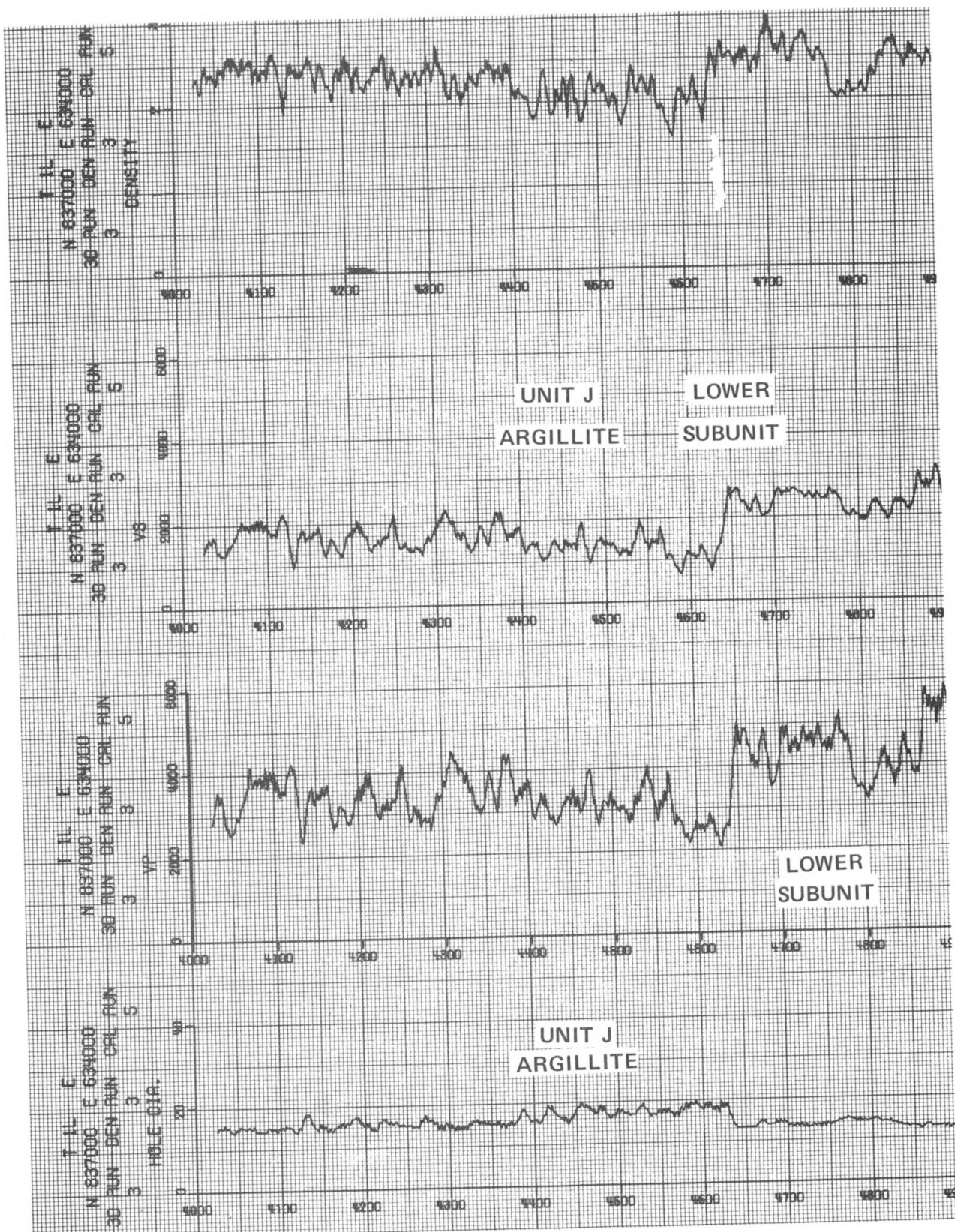


Fig. 6. Caliper, velocity, and density logs for borehole Uell. The depths logged are from 4300 to 4850 ft (1310.6 to 1478.3 m), and the argillite/lower-subunit boundary of unit J is at 4640 ft (1414.3 m).

beds. In the lower subunit of UelL the average V_p is 4.3 km/s, with a range of from 3.2 to 5.3 km/s. In the same locations, the average V_s is 2.4 km/s with a range of from 2.0 to 2.7 km/s. Figure 7 shows velocities (mainly Vibroseis^(R)) for the lower part of unit J, including the lower-subunit/argillite-unit boundary. Both the API neutron log and the Vibroseis^(R) log show the change from argillaceous argillite to siliceous argillite in the hole. In the argillite, V_p is about 3.0 km/s, and in the lower subunit it is about 3.9 km/s. The 3-Dlog records velocities up to 6 km/s in the limestone of unit I. In light of these data, the 3.70 km/s value for sonic velocity in the Eleana Formation, as given by McKague,¹ may be slightly high for the argillite. A more accurate value to use is from 3.0 to 3.5 km/s for zones of LQA and from 3.5 to 4.0 km/s for HQA. More refined velocity estimates for unit J can be obtained by the further reduction of log data from Uel7e, UelL, Uel7a, Uel6d, and Uel6f.

Because they contain a large amount of sheet silicate minerals, shale and argillite have anisotropic physical properties that are related to the degree of mineral alignment within the bedding plane. Velocity anisotropy data are not available for the Eleana Formation, but Jones and Wang⁴⁰ have found significant velocity anisotropy in wet samples of Cretaceous shale from the Williston Basin, in North Dakota. The shales that they examined had a mineralogy similar to that of the Eleana Formation argillaceous argillite (LQA). For samples taken from a depth of 5000 ft (1524 m), the V_p at 1 kbar (100 MPa) was 3.3 km/s parallel to, and 4.0 km/s perpendicular to, the bedding. For shear waves at 1 kbar V_s parallel to the bedding was 2.1 km/s, and V_s perpendicular to bedding was 1.5 km/s. The anisotropy was found to persist, decreasing slightly, to pressures of 4 kbar (400 MPa). Thus, a minimum of 10 to 15% anisotropy (isotropic within the bedding plane) could be expected for the Eleana argillite. Anisotropy of seismic velocity reflects inherent elastic anisotropy, which Terra Tek examined in samples from the Yacht hole. Mechanical tests were done by Terra Tek¹⁹ on samples from 4209 to 4230 ft (1282.9 to 1289.3 m) and from 5144 to 5155 ft (1567.9 to 1589.8 m) in the Yacht (UelL) hole. The results for one set of data, for six specimens from the 4216 ft (1285 m) deep unit J, are:

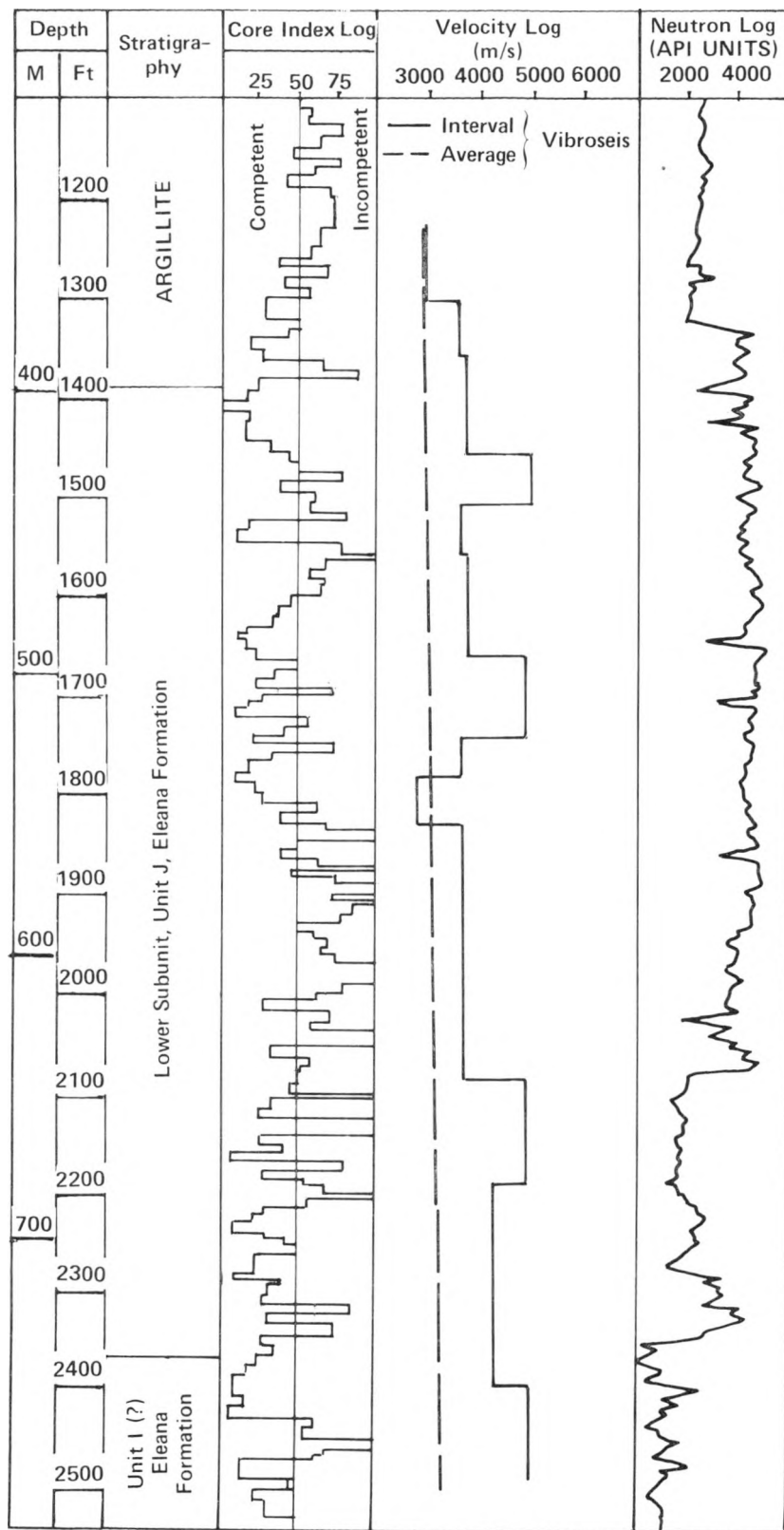


Fig. 7. Comparison of logs for borehole Ue25a-3.²⁹ The depths logged here are from 1100 to 2600 ft (335.3 to 792.5 m).

Bedding Plane	Apparent Young's Modulus (GPa)	Apparent Shear Modulus (GPa)	Poisson's Ratio (Calculated)
Angle			
Perpendicular	12.0	4.5	0.33
45°	16.0	7.5	0.07
Parallel	22.0	9.4	0.17

Tests to determine the differential stress at failure for confining pressures up to 4 kbar (400 MPa) showed no obvious dependency on bedding plane angle, and variations were attributed to lithologic variations.

Hydrostats (volume strains vs confining pressures) were determined by Terra Tek¹⁹ and compared with other shales. Their Fig. 5 is reproduced in Fig. 8 for reference. Triaxial extension tests were carried out by Terra Tek on the same Yacht hole samples. The results clearly indicated a noncentered yield surface about the hydrostat.¹⁹ Uniaxial strain tests were also done, to approximate the conditions found during shock loading, with much lower strain rates in the laboratory. The change of Poisson's ratio with mean stress in the uniaxial tests is shown in Fig. 9 (reproduced from Fig. 20 of the Terra Tek report¹⁹). Denny²⁷ used values of 0.27, 0.31, and 0.35 for Poisson's ratio in the SOC code calculations. Strain rate tests done between 10^{-4} s^{-1} to 10^2 s^{-1} revealed approximately a 20% increase in strength, per decade increase in strain-rate. A more complete discussion of the Terra Tek data is presented in Appendix A.

Mechanical tests were also done on cores from Ue25a-3 and Ue17e by Holmes and Narver, at the NTS. Data from Ue25a-3 are given in Table 3, a reproduction of Table 4 in Maldonado.²⁹ Hoover and Morrison¹² compared mechanical properties with the occurrence of HQA and LQA layers,

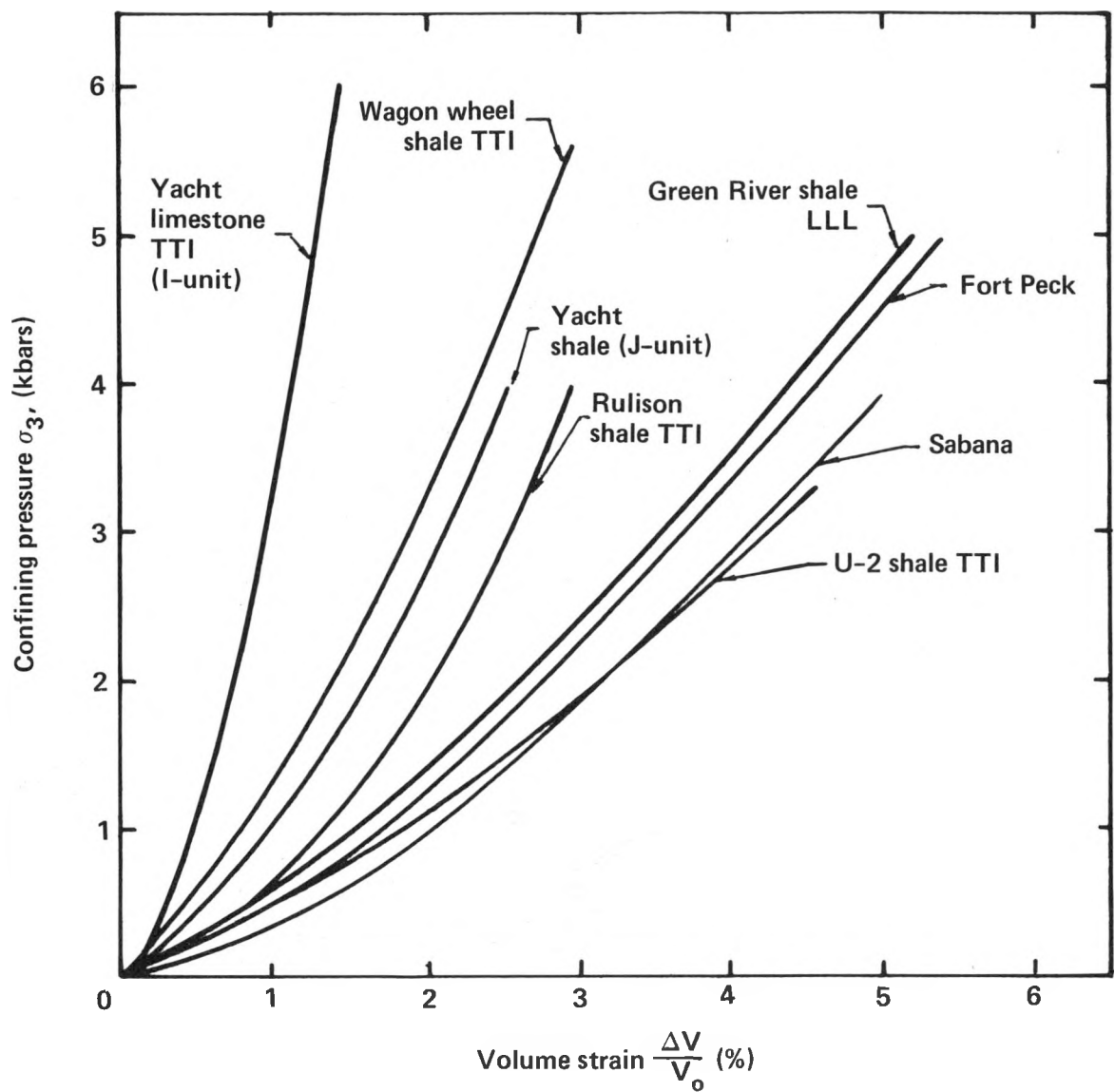


Fig. 8. A comparison of the hydrostats for various shales. (From Terra Tek.¹⁹)

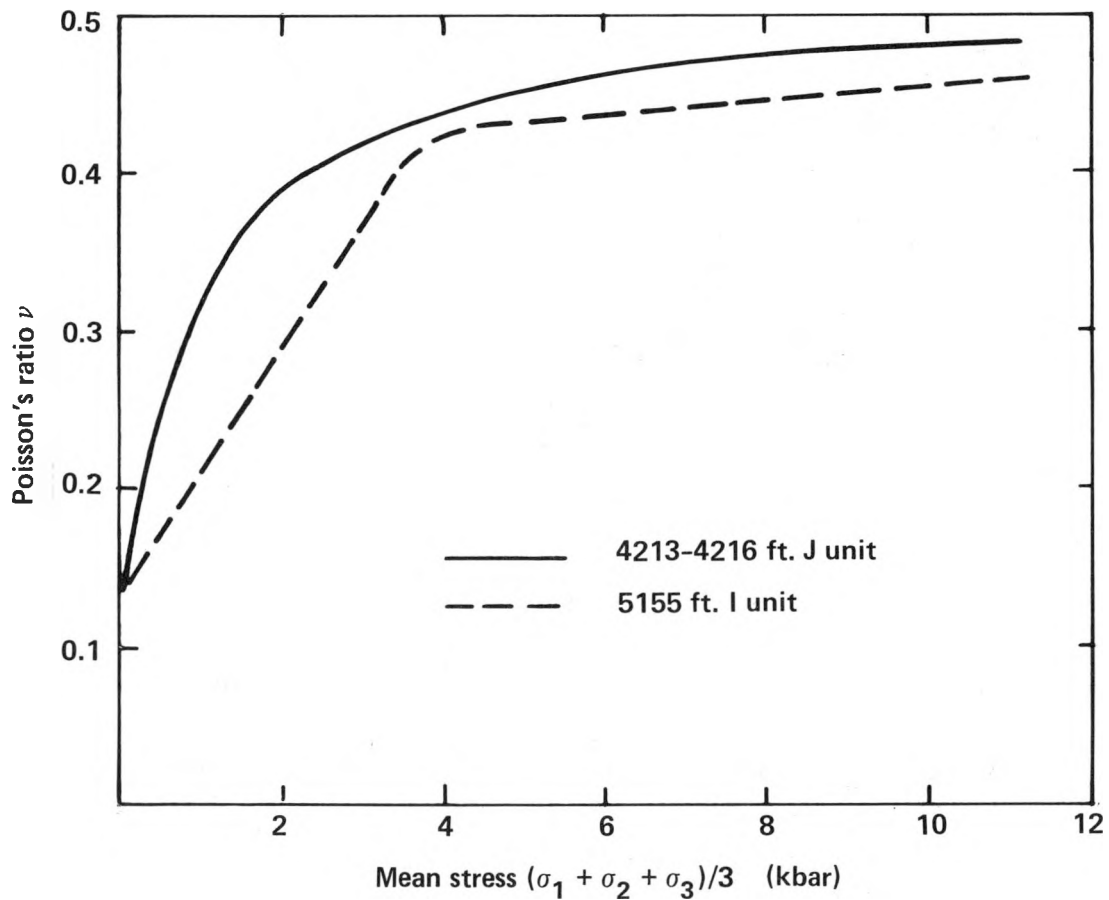


Fig. 9. Variation in Poisson's ratio with mean stress for the unit I limestone and the unit J shale. (From Terra Tek.¹⁹)

Table 3. Material properties determinations of cores from the UE25a drill hole. Measurements at zero confining pressure, by Holmes and Narver, Inc., Mercury, Nevada.

Depth		Axial Stress at Failure	Modulus of Elasticity $\times 10^3$ MPa	Poisson's ratio (v)	Bulk Modulus $\times 10^3$ MPa	Shear Modulus $\times 10^3$ MPa	Lithology
Metres	Feet	MPa	MPa		MPa	MPa	
293.2	962	12.55	9.19	0.31	8.63	3.74	Argillite
394.4	1307	9.10	4.34	0.15	2.08	1.88	Argillite
425.2	1395	37.50	46.40	0.22	27.17	19.10	Altered Argillite
441.9	1450	15.40	4.36	0.22	2.57	1.79	Alt. Argill.
466.0	1529	88.25	42.20	0.15	19.93	18.41	Alt. Argill.
505.1	1657	23.99	29.37	0.22	17.58	11.99	Alt. Argill.
523.3	1717	19.03	15.93	0.22	9.31	6.56	Alt. Argill.
591.3	1940	67.91	43.44	0.14	19.86	19.17	Alt. Argill.
634.9	2083	60.05	45.09	0.19	23.86	19.03	Meta- sandstone
675.1	2215	23.51	16.48	0.13	7.38	7.31	Alt. Argill.
700.4	2298	84.80	46.06	0.33	45.99	17.31	Alt. Argill.

The elastic constants were calculated at 50% of the failure stress. The bulk modulus equation is $E/3(1 - 2v)$. The shear modulus equation is $E/2(1 + v)$. E = the modulus of elasticity, and v = Poisson's ratio.

and a summary of their data from Uel7e is given below:

Property	HQA (15 Samples)	LQA (9 Samples)
	mean (range)	mean (range)
Unconfined Compressive Strength, in GPa	41.86 (23.34 - 64.20)	1.48 (0.23 - 4.15)
Young's Modulus, in GPa	12.24 (5.13 - 19.86)	1.25 (0.70 - 2.29)
Poisson's Ratio	0.26 (0.07 - 0.37)	0.34 (0.26 - 0.41)

The range of values is similar for both sets of data. The lower strength values given in Table 3 are similar to those of the LQA rock, although Hoover and Morrison¹² report that LQA zones were not found in Ue25a-3. The data clearly show that the LQA zones are an order of magnitude weaker.

The question of the distribution of LQA and HQA zones was addressed by Hoover and Morrison¹² for the Uel7e borehole. In some zones, the occurrence of LQA was very infrequent; typically one zone per 7.1 m. These zones are hereby referred to as HI zones (HQA frequent). In other zones LQA would occur as often as one zone per 1.9 m. These zones will be referred to here as LO zones (LQA frequent). In each case, the LQA zones are typically 0.5 m thick. The largest interval dominated by a HI zone (where LQA layers are less than 10%) was 157 m. The largest interval dominated by a LO zone (where LQA was greater than 20%) was 186 m. In general, these zones can be identified from velocity and API neutron logs.

The core was found to be highly fractured, with a highly variable core index. Both Uel7e and Ue25a-3 encountered numerous high-angle

faults and brecciated zones. In Ue25a-3 the average fracture frequency was 13.2 m^{-1} of which 66% were closed.²⁹ The core index (see Fig. 7) is highly variable, with roughly 50% of the rock classed as incompetent. The fracture frequency in Uel7e ranged from 1.4 m^{-1} , with most fractures being parallel to the bedding planes.¹² In Uel7e, 23 faults were noted: most are displaced only a few metres. The nature of shale and argillite is such that at depths of less than a few kilometres (in the brittle field) deformation will be accommodated primarily by bedding-plane slip, due to the thinness of individual bedding planes. Thus, it is to be expected that much of the fracturing noted in the core is probably due to minor local slip along bedding planes, and is not related to large-scale faulting. Deformational characteristics are discussed further in Section V.

Electrical, Thermal, and Hydrologic Properties

The electrical resistivity of the argillite is highly dependent upon the ratio of quartz to mica minerals. This makes the resistivity log a valuable tool for lithologic characterization. Argillaceous argillite has a resistivity that is generally less than 30 ohm-m, while that of siliceous argillite is greater than 50 ohm-m. Quartzite and limestone zones are marked by even higher resistivities. The usefulness of the resistivity log is dramatically demonstrated in Fig. 10, which illustrates a log from the 3600 to 5400 ft (1097.2 to 1645.9 m) level in UelL. Quartzite beds within the unit J argillite are easily detected; and the transition to the lower subunit (more quartzite and limestone rich), and to unit I below it, is quite marked. In the Syncline Ridge area,^{23,24,33} the contrasting resistivities of the argillite, compared to those of the over-and-underlying limestone and dolomite were used to map the subsurface argillite with electrical soundings.

The thermal properties of unit J were investigated with heater experiments by Lappin, et al.,³⁵ at depths of 25 m, near Uel7e. The thermal conductivity was found to be anisotropic. At 100°C , the axial conductivity was from $1.62 \text{ W/m}^{\circ}\text{C}$ to $1.73 \text{ W/m}^{\circ}\text{C}$, and the radial conductivity was $2.06 \text{ W/m}^{\circ}\text{C}$. They concluded that a strong coupling exists between the thermal and mechanical behavior of the argillite at elevated

COMBINE VERSION 1 COMPILED 06-08-77
RUN BY NORMAN AT U 11/06/81 14:11:02

UE1L ELECTRIC(64" NORM) RUN 2 8-7-72 1525-1705 B 3850-5113

DEPTH(FT) RESISTIVITY...OHM-M

DEMON-4 COMPILED 03-09-78 RUN BY NORMAN U 11/06/81 14:17:54
TOTAL SWAP = 0, DEL = 0, GAP = 9, RPT = 0, CHG = 0, DUP = 0, INDET = 0

-28-

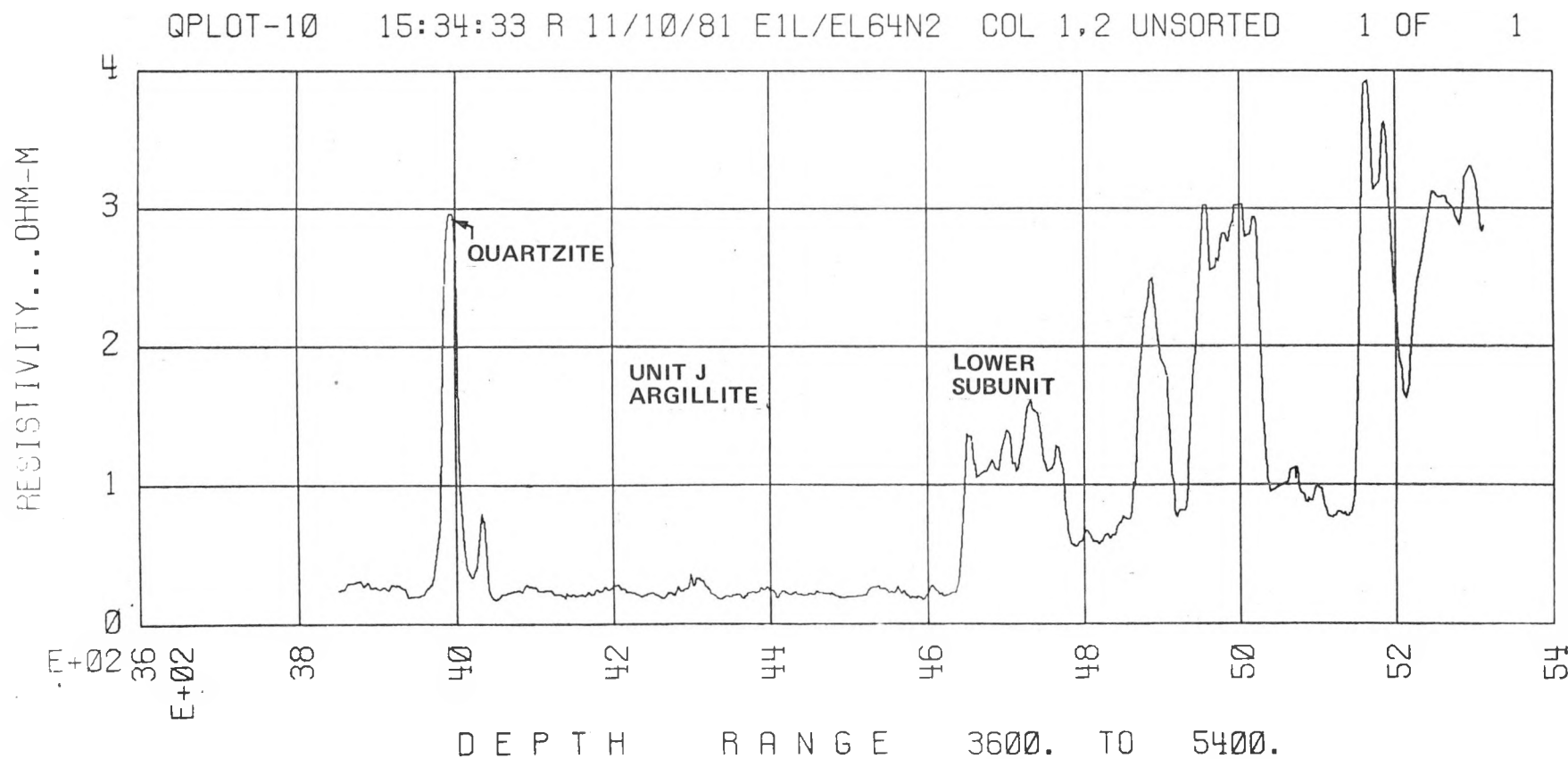


Fig. 10. Resistivity log for a portion of drill hole Ue1L. A quartzite layer occurs at 3990 ft, and the lower subunit starts at 4640 ft.

temperatures. A temperature log of the UelL hole⁴¹ revealed a gradient of 1.4 to 1.5°F/100 ft (0.78 to 0.83°C/30.5 m). For a surface temperature of 70°F (21°C), the temperature at the 4200 ft level would be 129° to 133°F (53.9 to 56.2°C)

Hydrologic data for the Syncline Ridge area were summarized by Dinwiddie and Weir.³¹ The Tippipah limestone overlying the Eleana Formation is highly transmissive, while the argillite and unfractured quartzite of the Eleana have extremely low permeability. A high hydraulic head was encountered in the Eleana, indicating a potential for upward flow.

Dinwiddie and Weir,³¹ Hoover and Morrison,¹² and D. O. Emerson (personal communication concerning UelL), have remarked on the difficulties of drilling in argillite. Most problems involve caving and erosion of the hole, which is often related to the presence of faults and fractures. Squeezing conditions were reported in Uel7e, in the upper part of the Eleana.³² Heavy drilling muds were often used to stabilize the hole. In general, it was difficult to keep the hole in gage when drilling in the argillite (see Fig. 6).

Summary

The Eleana argillite is a fine-grained anisotropic rock, with a low porosity and an extremely low permeability. Its sonic velocity and mechanical properties are anisotropic, with an order of magnitude variation in strength between zones that are high in LQA and those that are low in LQA. Sonic velocity, API neutron, and resistivity logs all clearly indicate the separations between the LQA, HQA, and the quartzite/limestone lithologies.

V. STRUCTURAL SETTING OF THE ELEANA FORMATION

The Paleozoic rocks at the NTS were deformed in pre-Cenozoic time by thrust faulting with accompanying folding, strike-slip faulting, and normal faulting. Barnes and Poole⁴² identified two thrust-fault systems. These are the Tippinip thrust, in which upper Precambrian and

lower Paleozoic rocks are thrust to the southeast over upper Paleozoic rocks, and the Mine Mountain CP thrust, in which Devonian and Silurian rocks have been thrust southeastward over the Eleana Formation and Tippipah limestone. Barnes and Pool also suggest⁴² that a thrust sheet of Cambrian rocks in the Spotted Range (east of the NTS) is part of the CP thrust seen in the CP hills. Sinnock² has proposed that the thrusting consists of three separate belts (Fig. 11) with separate roots to the thrust systems. Sinnock uses the names (west to east), Mine Mountain, CP-Tippinip, and Spotted Range to refer to the thrust zones. The Eleana Formation and the Pennsylvanian Tippipah limestone formed the basal plane for the Mine Mountain and CP thrust structures. Sinnock² states that the Eleana Formation provided the basal slip surface for thrusting. Locally, in the Eleana Range, the Eleana Formation has thrust faults within it and contains tight, overturned folds in areas caught between upper and lower bounding thrust faults.

In order to better understand the general structural setting of the Eleana Formation in the region surrounding Yucca Flat, geologic maps of the Mine Mountain, Eleana Range, western Yucca Flat, Rainier Mesa, Oak Spring, Oak Spring Butte, and Belted Peak areas were examined, and preliminary cross-sections were prepared with a restoration of the Cenozoic fault movement. Before discussing the results of this study, a brief tutorial on our current knowledge concerning thrust faulting and deformation mechanisms will be presented for the benefit of the general reader.

Characteristics of Thrust Faulting

The term "thrust fault" refers to any contractional fault,⁴³ and the term, "thrust sheet" refers to any rock mass carried upon a thrust fault. Rocks above the thrust surface are called the "hanging wall;" those below it, the "footwall." A typical cross section of a thrust fault is shown in Fig. 12. The areas at the extreme right and left of the figure, where the sediments are still lying flat, are called "flats." Bedding planes in these zones can be used as arbitrary datum surfaces. Between the two flats, the area where layers cut up-section is called a "ramp." Ramps cut off arbitrary datum surfaces and result in a net crustal shortening. In

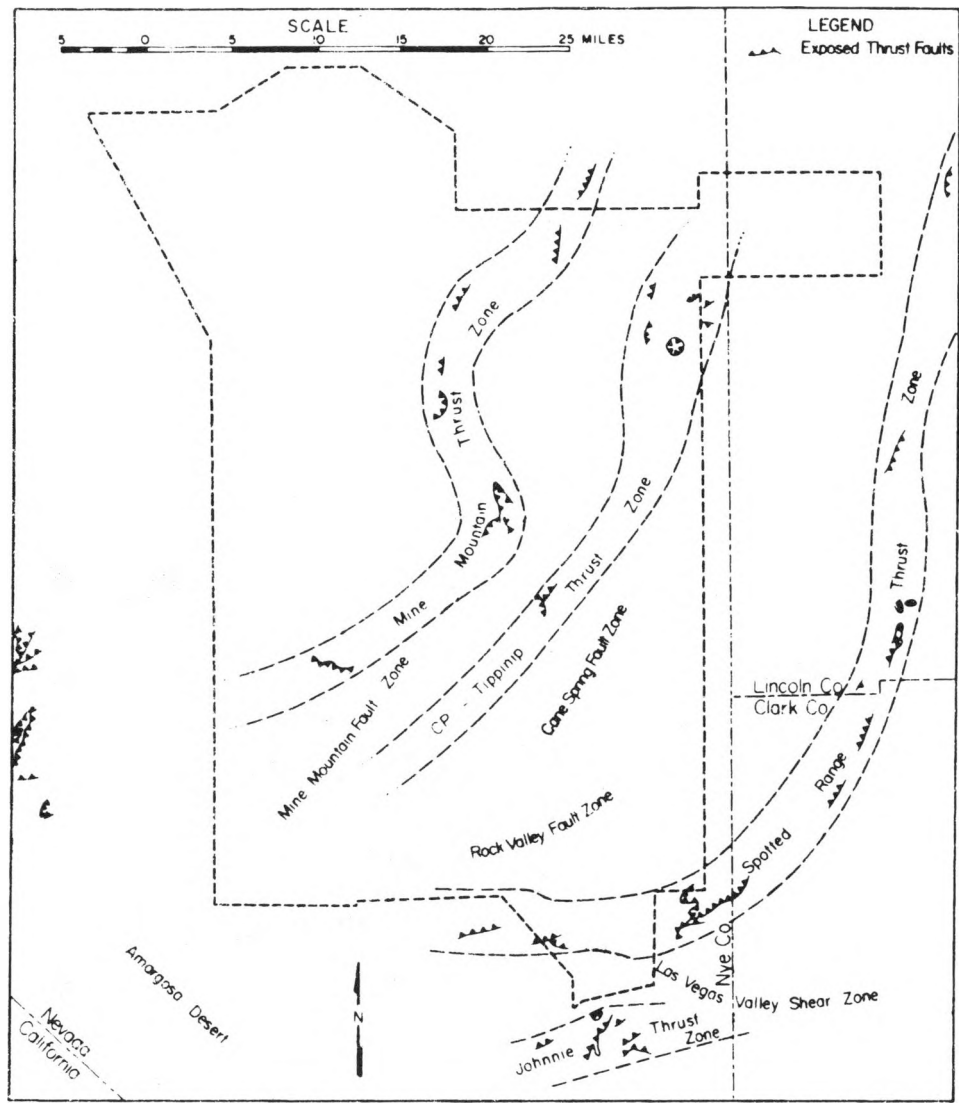


Fig. 11. Location of major thrust zones in Paleozoic rocks in the NTS region (after Sinnock²).

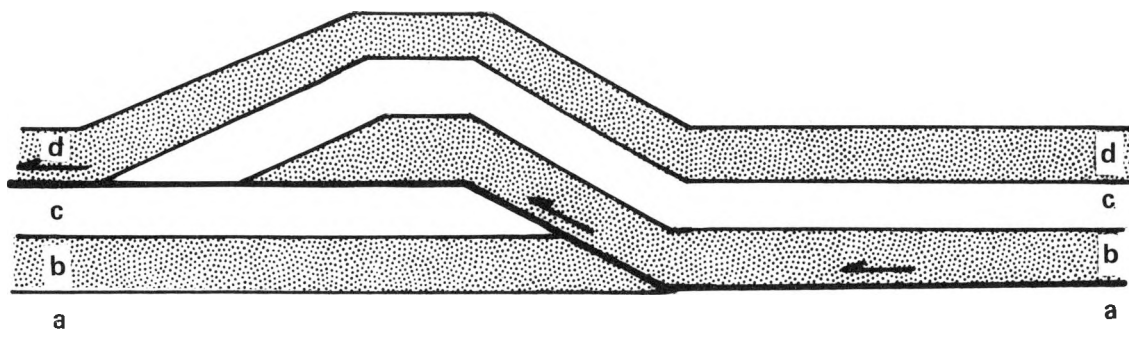


Fig. 12. Idealized diagram of thrust fault geometry (after Butler⁴³). The dark line is the fault plane.

Fig. 12, strata b, c, and d are folded above the ramp, forming what is called a "blind thrust," because it does not break through to the surface. The contacts between units a and b on the right, and between units c and d on the left, are fault surfaces where movement has occurred on a plane parallel to the layering. Such bedding-parallel surfaces may be difficult to recognize in the field without knowing that ramps exist nearby.

Two types of displacement sequences can arise. One occurs when a younger thrust develops in the footwall of an earlier thrust; the second, when the younger fault is in the hanging wall of the older thrust.⁴³ The first type (shown in Fig. 13) is called piggy-back thrust propagation. The second type (shown in Fig. 14) is called an overstep or overlap sequence.⁴³ Piggy-back thrust sequences can develop into imbricate stacks or "schuppen" structures, in which slices of displaced rocks are caught between upper and lower bounding thrusts, as shown in Fig. 15. This type of structure, sometimes called a duplex, consists of a series of thrust slices ("horses") caught between a roof thrust and a floor (or "sole") thrust.⁴³

Thrust faults do not cut through the same strata along strike. This results in differential amounts of stacking, with a concomitant folding above the ramps, as well as the development of monoclines with axes parallel to the direction of transport. When the differential offset of various sections in a thrust sheet occurs, the movement will be accommodated along faults that form nearly parallel to the movement direction. Such faults will display strike-slip as well as vertical displacements. Sometimes thrusts at higher levels can be related to the accommodation of folds above a ramp or other geometries. Examples of an out-of-syncline thrust and a pop-up back thrust are shown in Fig. 16. For further discussion of thrust fault geometries and methods for analyzing structures, the reader is referred to Dahlstrom,⁴⁴ and Elliott and Johnson.⁴⁵

Eleana Formation rocks at the NTS are of a low (greenschist or lower) metamorphic grade.¹² They have not therefore been deeply buried. The thrust faulting probably occurred near the surface, and deformation would most likely have been in the brittle mode. The pervasive fracturing and the evidence of localized slip on bedding planes in the argillite (as seen in the drill cores) confirms that bedding plane slip is a primary deformation mechanism in the Eleana Formation. The amount of shortening that can be accommodated by bedding plane slip (in which all the deformation occurs as a

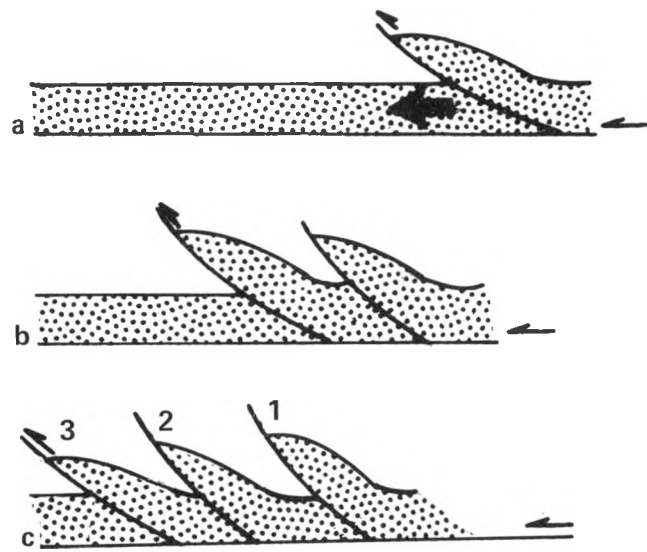


Fig. 13. Sequential development of a piggy-back thrust sequence. The large arrow shows the direction of thrust propagation. (After Butler.⁴³)

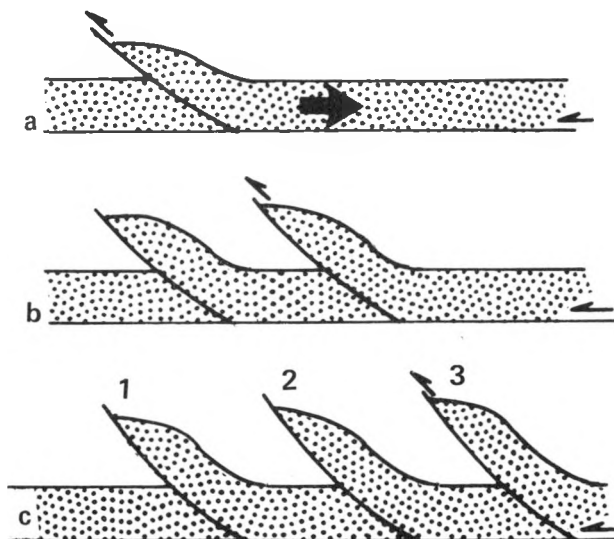


Fig. 14. Sequential development of an overstep thrust sequence. The large arrow shows the direction of thrust propagation. (After Butler.⁴³)

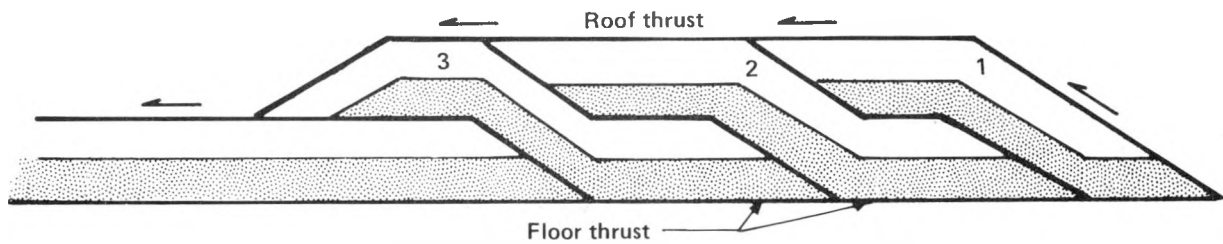


Fig. 15. A cross section, parallel to the transport direction, through a duplex. The horses are numbered 1 to 3, in the order of their development.

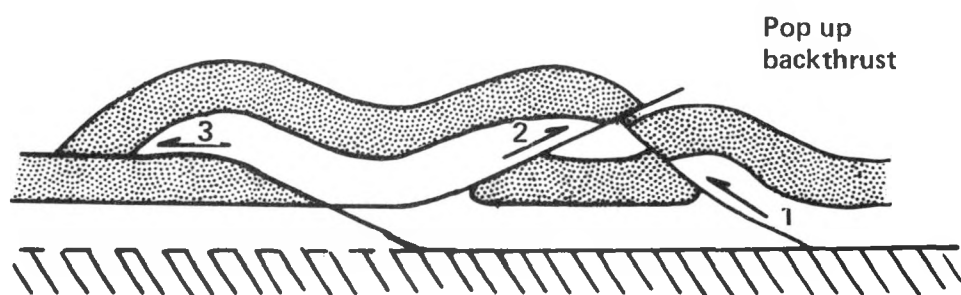
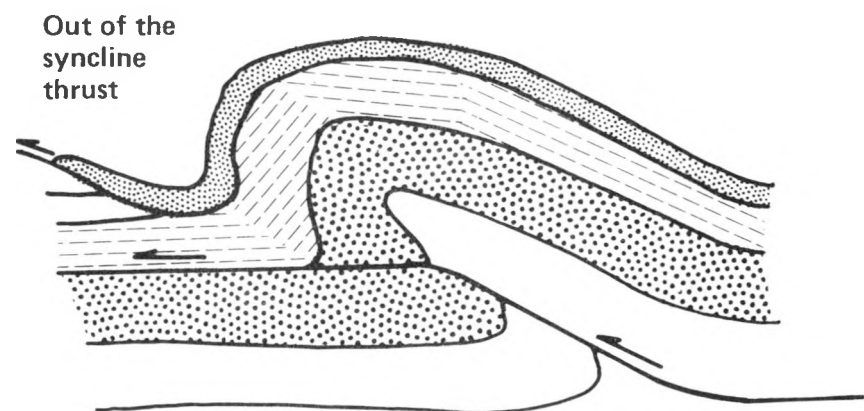


Fig. 16. Examples of an out-of-the-syncline thrust and a pop-up back thrust. The numbers indicate the sequence of thrusting. (From Butler.⁴³)

slip between layers, with no intralayer deformation) is directly related to bedding plane thickness.⁴⁶ The Eleana Formation's argillites are much more thinly bedded than the carbonate or quartzite units above and below, and would therefore be expected to deform more easily. The author has observed small-scale chevron folds (with amplitudes of 15 cm or less) in unit H argillite (as mapped by Hoover and Morrison¹²) in the Red Canyon area of the Eleana Range.

When large-scale buckling occurs in bedded units under brittle conditions with flexural-slip folding, in which the bedding plane thickness remains relatively constant, accommodation problems develop in the core of the folds. Space is usually accommodated by faulting along arcuate thrust planes.⁴⁷ An example of thrust faults developed between the layers of folded sedimentary rock is shown in Fig. 17. These types of faults would be expected to be common within the large-scale folds in the Eleana Formation.

Recent studies of other pre-Cenozoic thrust faults south of the NTS⁴⁸⁻⁵¹ have revealed certain features that may be worthy of consideration in evaluating thrusts at the NTS. Studies of the Keystone/Muddy Mountain/Glendale thrust system, and of the underlying Contact/Red Spring/North Buffington/Mormon system in the Spring and Muddy Mountains, reveal that thrusting occurred at a very shallow crustal level. Specifically, the zone of failure occurred within competent dolomite layers; rather than in the shales (which occur only a few hundred metres below the thrust plane). This contradicts the general assumption (and that made by Sinnock,² and Barnes and Poole,⁴² about the Eleana Formation) that the weakest stratigraphic units always provides the area where fracturing always occurs in thrusting.

A key question concerning the position of the Eleana Formation with respect to structures developed during thrust faulting is whether the degree of internal deformation is related to the position of units within a thrust system. Brock and Engelder⁴⁸ observed that deformation offsets can extend more than twice as far above a thrust plane as below it. Thus, it would be expected that deformation features such as cataclasis, shearing, fracturing, or folding would be more intense above a thrust sheet. Knowledge of the position of various units with respect to the flats, ramps, and folds in a thrust system may lead to a better assessment of the degree of internal deformation. With these concepts in mind, a cursory study of structural features of the Mine Mountain/CP-thrust system was carried out.

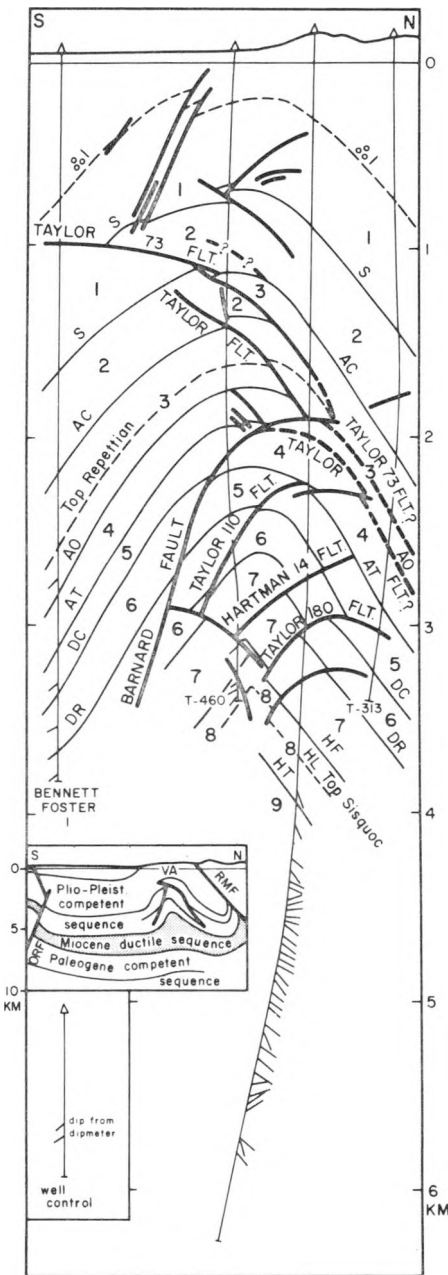


Fig. 17. An example of fault formation in the interior of folds that accommodate strain without flow. The sedimentary layers are numbered 1 through 9, and the heavy lines are faults. This is a north-south cross section across the Ventura Avenue anticline, near Ventura River, California. (After Yeats.⁴⁷)

Structural Setting of the Western Side of Yucca Flat and Areas to the North and South

A structural section of the Mine Mountain/CP Hills area (after Barnes and Pool⁴²) is shown in Fig. 18. Note that the Eleana Formation is only mildly folded beneath the CP thrust. The thrust also cuts upward into the Tippipah limestone in the CP Hills. Another interpretation of the geology across the NTS is provided by Sinnock.² In Fig. 19, Cenozoic units have been removed and the Cenozoic fault movements have been restored on Sinnock's cross section (B-B', pp. 31-32) from Bare Mountain, across Mid Valley and Yucca Flat, to the Pintwater Range. There are three thrust faults shown, with the greatest offset of strata occurring on the two westernmost faults. The faults have true dips of from 10° to 15°, with the easternmost fault having the least dip. Note that the Eleana Formation, as depicted in Fig. 19, is tightly folded beneath the thrust in the Yucca Flat area: this corresponds to the Syncline Ridge structure. A large overturned fold is depicted in the Eleana Formation above the thrust between Mid Valley and Yucca Flat: this corresponds to the tight, overturned folding seen in the Eleana Ridge area.⁸⁻¹⁰ The proximity of the Mine Mountain/Yucca Flat area to the thrust, coupled with the style of folding, suggests that the Eleana Formation would be more deformed or disrupted there than at the Calico Hills. However, a Tertiary intrusion at depth below the Calico Hills may account for the higher degree of fracturing seen in the cores from UE25a-3. It is also possible (D. Hoover, private communication) that the Mine Mountain area may have been affected by a similar intrusion.

A study was made of the progression of thrust-fault geometries from the Oak Spring Butte quadrangle (north of the NTS) south through the Mine Mountain quadrangle. Geologic cross sections from the USGS's 7.5-minute geologic map series were restored to the pre-Cenozoic state by removing tuff units and restoring movements on Cenozoic faults. These simplified cross sections are assembled in Fig. 20.

In the Oak Spring Butte and Oak Spring quadrangle cross sections of Fig. 20, rocks of Cambrian through Devonian age have been upthrust along two ramps. However, the two westernmost faults in the area are gravity slides, in which younger formations (such as the Eleana) have been dropped down along low-angle (listric-normal?) faults. The overturned fold in the Eleana in the

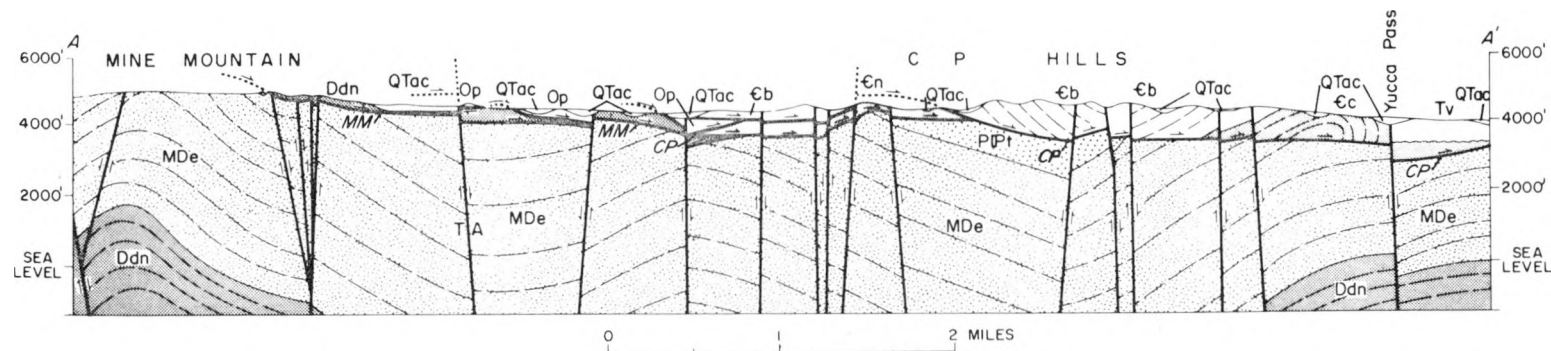


Fig. 18. A west-east structural section from Mine Mountain to Yucca Pass, at the NTS (after Barnes and Poole⁴²). Key: MDe - Eleana Formation, PIpt - Tippipah limestone, Ddn - Devonian carbonate, Eb and Ec - Cambrian rocks. The symbol CP identifies the location of the CP thrust.

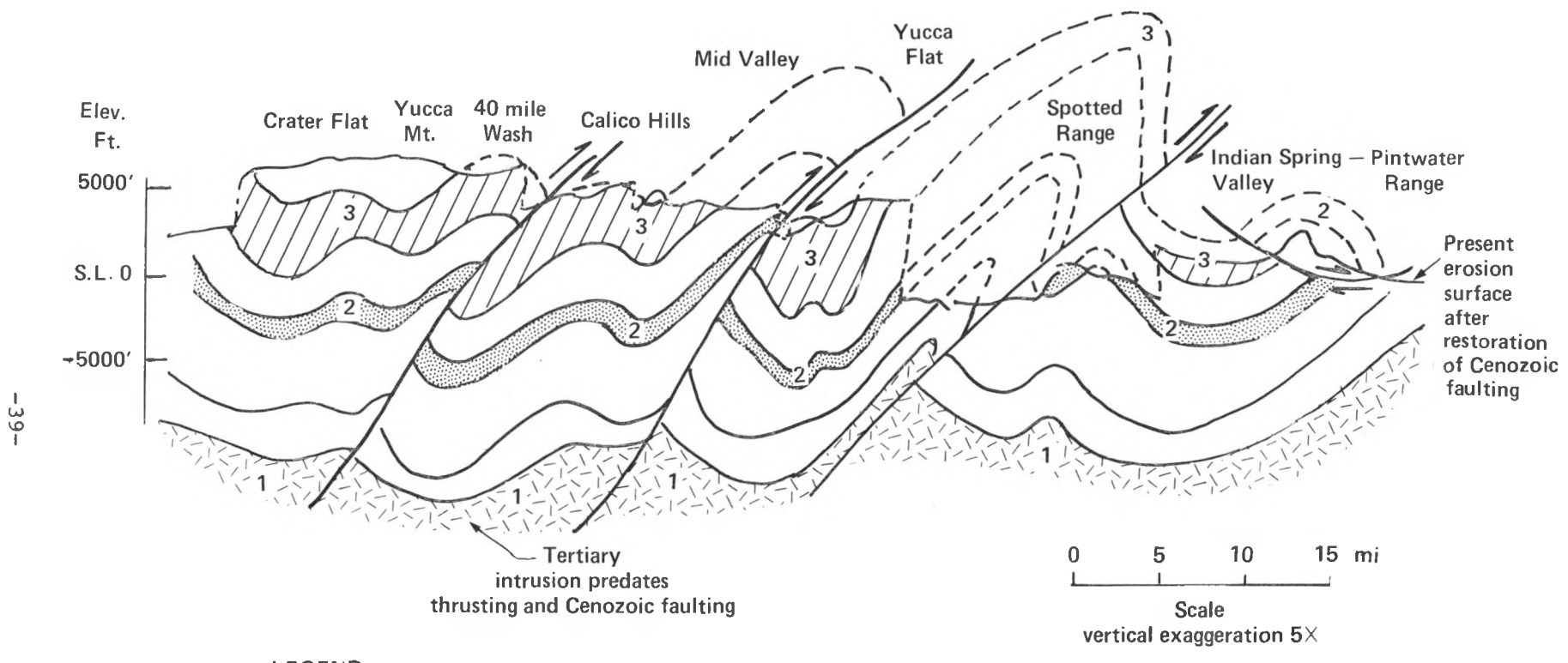


Fig. 19. A cross section across the NTS, from Bare Mountain to the Pintwater Range. Cenozoic tuff deposits have been removed and movement on Cenozoic normal faults has been restored. (Modified from Sinnock.²)

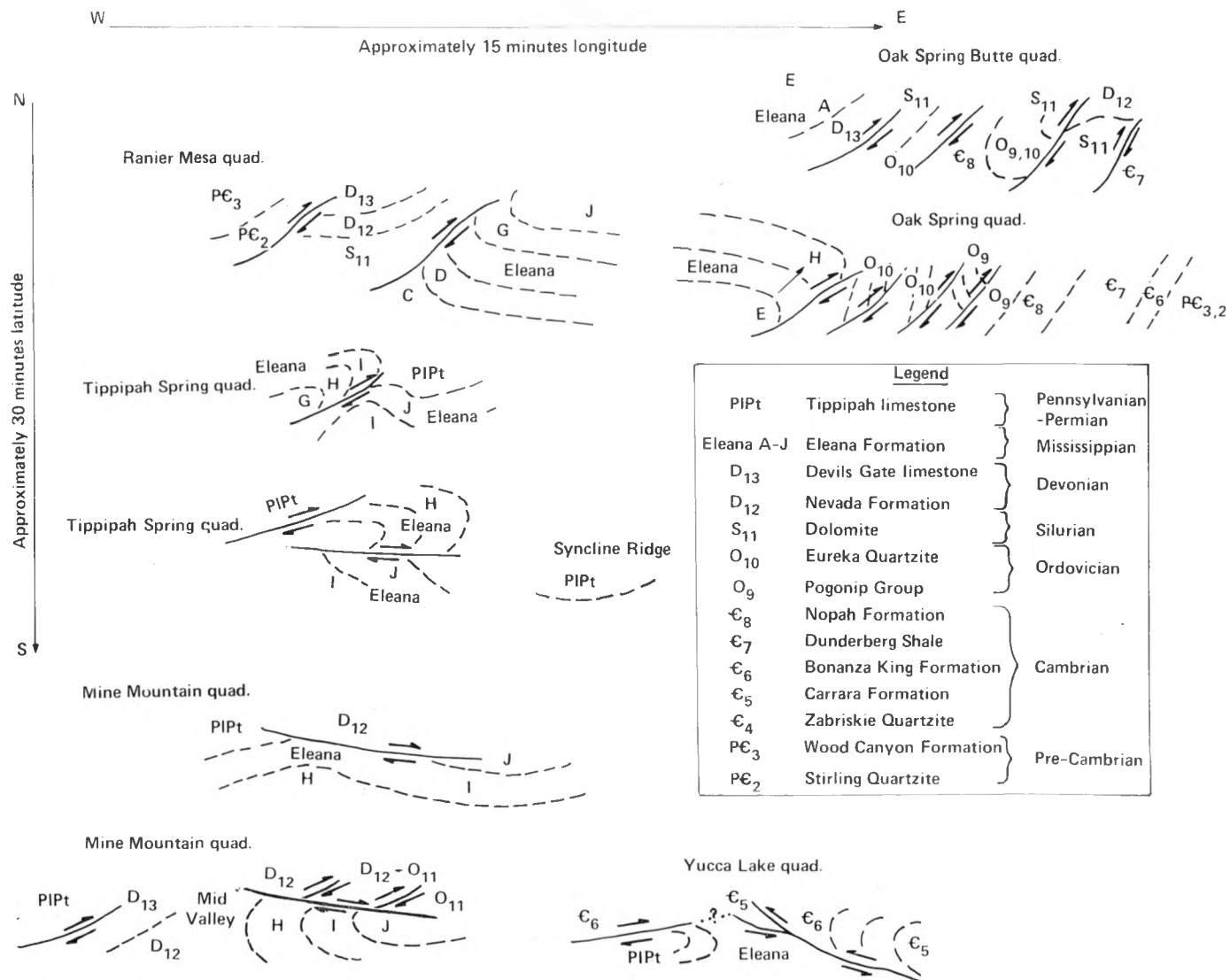


Fig. 20. Diagrammatic cross sections (not to scale) of the NTS/Nellis AFB area, illustrating the structures found in Paleozoic formations. The Cenozoic tuffs have been removed and normal fault movement has been restored.

Oak Spring quadrangle has probably been dropped down from a higher level, and the steeply dipping Ordovician rocks below the fault are probably part of the overturned limb of the same fold. The easternmost faults appear to be part of an overlap sequence.

In the Rainier Mesa quadrangle cross section, shown in Fig. 20, two ramps are seen. One consists of Precambrian rocks over Silurian and Devonian rocks: the other carries Silurian-Devonian rocks over the Eleana Formation. The upturning of Eleana Formation rocks toward the fault suggests that a large overturned fold above the thrust has been eroded away. To the east, away from the thrust, the Eleana Formation is relatively undeformed beneath the northern part of Yucca Flat. Sections in the Tippipah Spring quadrangle show thrusts between the Tippipah limestone and the Eleana Formation, and within the Eleana. A thrusting of the Tippipah over the Eleana is generally difficult to recognize because the contact is also a normal stratigraphic one. In the northern part of the Tippipah Springs quadrangle, especially near Red Canyon in the Eleana Ridge, a large overturned anticline occurs in the upper part of the Eleana Formation above a thrust. These faults may be smaller, imbricate structures, caught between lower-bounding (possibly, the CP thrust) and upper-bounding (Silurian-Devonian over the Eleana) thrusts, making the structure here a duplex. To the east, the Tippipah limestone and the underlying Eleana are less deformed below the thrust seen at Eleana Ridge (although Hoover and Morrison¹² have found evidence for thrusting at depth).

In the Mine Mountain and Yucca Lake quadrangles, the structural relations are puzzling. Imbricate thrusts occur within Ordovician-Devonian sequences, which in turn appear to have slid to the east over synclinally-folded Eleana Formation rocks in the Mine Mountain area. In the Yucca Lake area, Cambrian rocks are thrust over the Eleana and Tippipah to the west (a ramp), and appear to have slid downslope to the east. Another possible explanation could be that the folding of a previous thrust was accompanied by some sort of backthrusting.

The cursory examination just given cannot begin to satisfactorily unravel the structural complexity of the area. But by using diagrams such as those in Fig. 20, basic relationships can be worked out, and thrusts of a similar style can be correlated. Once exposure-level structures are better understood, a better insight can be gained into the Paleozoic sub-surface structure in areas such as Yucca Flat and Mid Valley. A valuable tool in structural analysis is

the dipmeter log, and the visual logging of dips from cores. As seen in the northern part of the Tippipah Spring quadrangle in Fig. 20, there is a sharp change in dip between beds of the overturned limb of the overlying thrust sheet and the beds below. A similar sharp change in borehole-log dips should be a clue to the location of a possible thrust fault.

The previous analysis was based solely on published cross sections from geologic quadrangle maps. In general, a geologic map represents reliable data based upon field observations. However, in many respects a geologic cross section is interpretive. Thrust faults need not be the primary element in the structural make-up of pre-Cenozoic rocks at the NTS. An interpretation emphasizing folding and down-playing thrust faulting might also fit both the geological and geophysical data.⁵² Robinson's⁵² interpretation of pre-Cenozoic structure sees the whole NTS region as a large asymmetric basin with steep sides to the west and south. Interior to the basin are smaller folds with wavelengths of a few miles. Some of the smaller thrust segments, such as the Mine Mountain and CP thrusts, are seen by Robinson as small gravity slides from the sides of synclines. The main point here is to emphasize that the data base for structural information is meager, and that widely divergent interpretations (consistent with the observations) are possible. An assessment of these interpretations is beyond the scope of this report.

Assessment of Sites Appropriate for Underground Testing in Argillite

Without knowing the detailed specifications needed for a particular test, only very generalized criteria can be used for site selection. For this general study, the following criteria are used to rank sites for suitability:

- Moderate topographic slopes
- An argillaceous argillite unit with adequate thickness
- A depth to the working point of less than 1000 m
- No proximity to large faults
- A minimal amount of internal structural complexity

Using these criteria a series of sites were considered, which are discussed in this section in terms of their relative suitability.

The Syncline Ridge Area. Figure 21 is an isopach map of the unit J argillite subunit from Hoover and Morrison.¹² Mesozoic and younger high-angle faults are also shown. From an examination of Fig. 21, some areas might be eliminated as being structurally too complex. These include the areas north of N262000 m and south of N254000 m. In between them, there are small areas east and west of Syncline Ridge with an adequate thickness of argillite and a minimum of structural complexity. Areas west of Syncline Ridge and east of the Eleana Range may be too topographically rugged to be suitable. Note, however, that the isopach map is based solely on electrical soundings, with little control from boreholes.

The Mid Valley Area. At the west side of the northern part of Mine Mountain, in Mid Valley, it can be inferred that the Eleana argillite occurs at depths of less than 1000 m. Little is known about the extent of Cenozoic faulting in the area, but pre-Cenozoic structures should not be very complicated, because unit J of the Eleana is seen to be gently dipping to the west on the western side of Mine Mountain.⁸ In the southern Mid Valley area, a ENE-trending fault has brought up Devonian carbonates, and the Cenozoic deposits are thicker.⁷ The Eleana Formation probably occurs below a thrust at the base of the carbonates (as it is seen in the CP Hills to the east⁷), but it may prove to be at a prohibitive depth for testing.

The Calico Hills Area. In the Calico Hills area of Jackass Flats, unit J of the Eleana Formation probably covers a large area of the subsurface at reasonable depths. However, little is known of the subsurface Cenozoic structure in the area, and the drill-hole core from the Ue25a-3 hole was found to be highly fractured.

The Yucca Flat Area. Probably the most promising area for testing sites is along the western side of Yucca Flat, especially in the northern part. In the Rainier Mesa quadrangle,¹⁰ the Tippinip fault marks a major boundary between the Eleana Formation and older Devonian/Ordovician carbonates and clastics. This boundary extends to the south, under Yucca Flat, to the west of the Yucca fault. The Tippinip fault may be a thrust, because the Eleana Formation is overturned, with tight folds near the contact. Possibly the fault was reactivated as a normal fault in Cenozoic times. In any case,

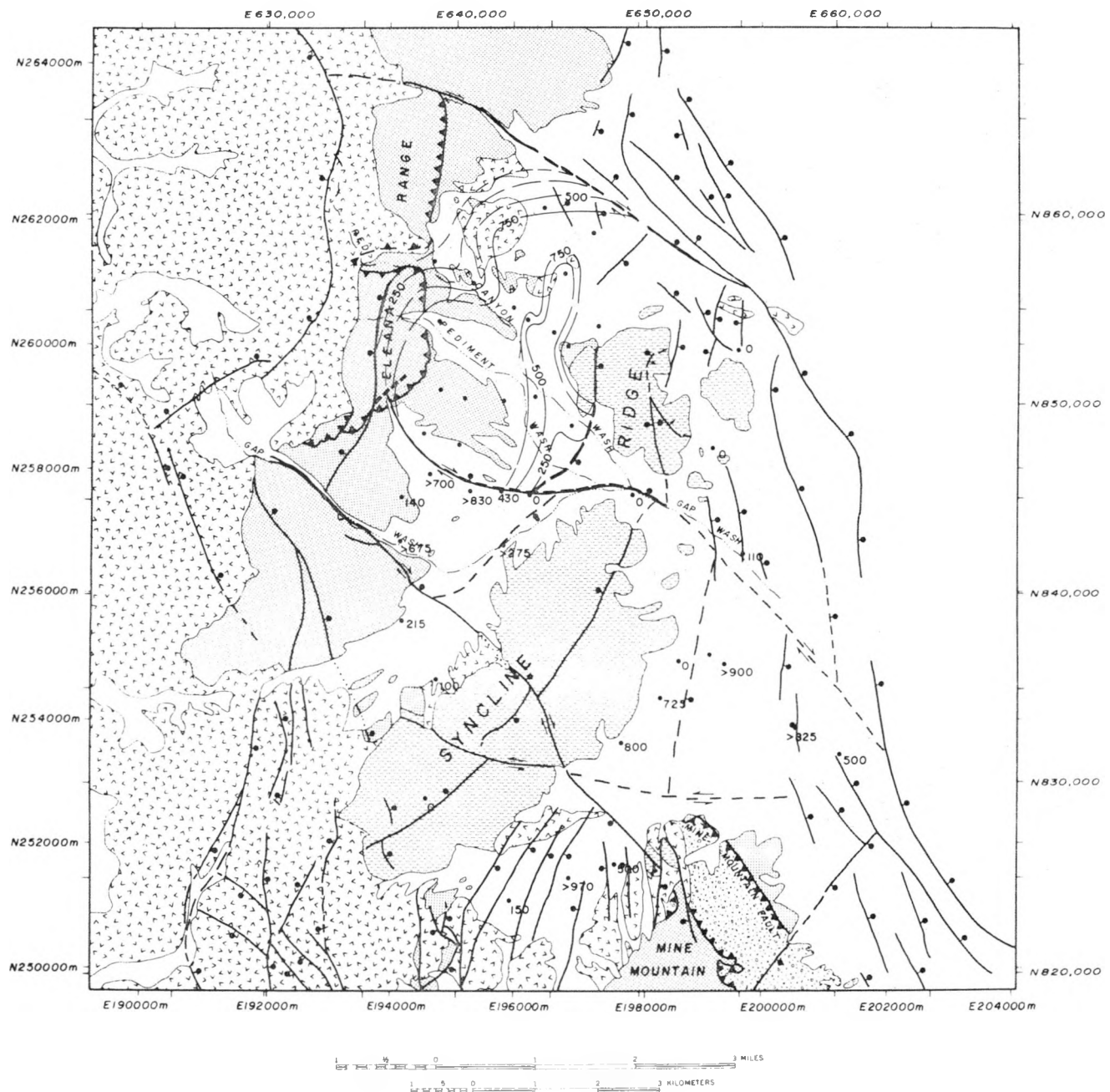


Fig. 21. An isopach map of the argillite subunit, with a contour interval of 250 m. The map is derived from geoelectrical sections computed from Schlumberger vertical electrical soundings (VES). The Argillite subunit of unit J in the Eleana Formation is defined as a continuous geoelectrical section, with a resistivity of less than 70 ohm-m. (From Hoover and Morrison.¹²)

the fault extends to the south and may be associated with the gravity high in Yucca Flat, which marks the place where lower-level basement rocks are closer to the surface. The contact can be tentatively located from drilling information, although confidence in the identification of Paleozoic rocks is minimal from the borehole data.

In Area 8, boreholes Ue8a-5, Ue8a-4, and Ue8a-11 all encountered argillite at depth, but no argillite was encountered to the east of these holes. In this area, the top of the Eleana is 300 to 400 m below the surface, and would probably be unit J, as the rocks in the Eleana Range to the west are dipping eastward. Without more detailed information about the subsurface Paleozoic rocks in Area 8, such as knowing whether the carbonate rocks to the east are Tippahah limestone or older mid-Paleozoic carbonates, only the western half of Area 8 appears suitable for finding argillite of unit J at acceptable depths.

Area 2 and Area 4 are similar to Area 8, although more is known about the subsurface geology in Area 4 (McArthur¹¹). In Area 2, the probable trace of the Tippinip fault swings to the east. Eleana formation rocks were found in Ue2b, Ue2a-1, Ue2dy at depths of from 600 to 1000 m. This suggests that some east-west trending normal faults may possibly exist between Areas 2 and 8. The Eleana Formation probably occurs beneath most of the western three-quarters of Area 2. In McArthur's¹¹ sections, it is also shown beneath most of Area 4, but the Eleana Formation has been confirmed as existing in the subsurface only in holes Ue4af, Ue4ab, and T.W.-D. West of the gravity high, the Eleana Formation lies either directly below Cenozoic deposits or Tippahah limestone. East of the gravity high the Eleana lies below undivided (unidentified?) Paleozoic carbonates (perhaps Tippahah?) and the inferred C.P. thrust plane. Structural details in the Paleozoic rocks beneath Area 4 are by no means well understood, and this is the best known part of Yucca Flat! Until more is known about subsurface Paleozoic stratigraphy and structure, the best area for siting tests would probably be in the western two-thirds of Area 4.

Area 6 is probably underlain by Cambrian rocks. The Eleana Formation probably underlies the Cambrian here, possibly beneath Tippahah limestone. However, not enough is known of the subsurface to make this area a good choice for a testing site. The western side of Area 1 has

been well characterized by Hoover and Morrison,¹² and Emerick.^{25,26} An adequate thickness of argillite is present at depths of 200 m or less (e.g. at the Yacht hole - Uell), but the presence of faults with large throw complicate things. Between Uelb and Uelc¹² a fault drops the Eleana Formation down to the east by over 700 m. Although more needs to be done to characterize the extent of this faulting, the area near Uell and a kilometer or so east of it should be adequate for testing.

Summary

The most promising areas for finding suitable amounts of argillite for underground testing are the western parts of Areas 1, 2, 4, and 8, with Areas 1 and 4 being somewhat better than 2 and 8. Two small areas between Syncline Ridge and the Eleana Range, between N256000 m and N261000 m, may also prove to be suitable.

VI. Conclusions and Recommendations

As a result of the Yacht (Plowshare) and Waste Isolation programs, the Eleana Formation's properties have been well characterized. Its composition is primarily quartz, illite, chlorite, and montmorillonite with minor carbonate. The argillite units characteristically have less of a quartz fraction, a higher mica fraction, and a very low carbonate content. The Eleana's physical properties reflect lithologic variation with depth, and logging tools (such as API neutron, 3-D velocity, and resistivity) are quite diagnostic in characterizing such changes. The areal variation in composition is probably not pronounced, although the data set is not complete enough to adequately assess this factor. There is a high probability that with adequate log data, correlations between boreholes will not be difficult. The argillite's mechanical properties are quite variable, but they can be predicted with the help of acoustic and electrical logging.

The biggest unknown with regard to the Eleana Formation is its structural complexity and the nature of its internal disruption. In terms of containment or testing parameters, this may prove to be an

unimportant factor. However, should structural factors prove to be important, a much better understanding of Paleozoic structure in the Yucca Flat area will be required. The nature of Paleozoic structures can only be adequately determined by thoroughly studying the entire area, not by focusing on one particular area. Every attempt will have to be made to positively identify the Paleozoic lithology in drill holes (e.g. a Pennsylvanian or Devonian carbonate, rather than a "Paleozoic carbonate"). Detailed electrical soundings should prove useful for characterizing the location of Eleana argillite units in the subsurface. Finally, and perhaps this should be the place to begin, the lithologic markers in the data base should be updated. This information is available for many holes, most notably in References 11, 12, 25, 26, 31, and 36.

ACKNOWLEDGMENT

Much of the information in this report was compiled by D. O. Emerson in a file on the Yacht project. His generous loan of the entire updated file considerably decreased the data assembly time for this report.

APPENDIX A

SOC CALCULATIONS FOR ELEANA FORMATION, UNIT J

Report by M. D. Denny
UOPKL 72-60 Memorandum to D. O. Emerson
Dec. 5, 1972

LAWRENCE LIVERMORE LABORATORY
K-Division, Bldg 121 L-47

December 5, 1972

UOPKL 72-60

M E M O R A N D U M

TO: Distribution
FROM: M. D. Denny
SUBJECT: SOC Calculations of the Dynamic Behavior of Yacht Rock

Described in this memorandum are the physical properties of the shale at the Yacht site and the ground shock environment in the shale as predicted by SOC code calculations for 30 and 100 kt explosions. Selected parameters as a function of range are compared with those of a 100 kt explosion in Wagon Wheel rock.

Material Properties

The material properties reported here are from measurements made by Terra Tek, Inc. (T^2) and by R. Schock of this laboratory on samples taken from approximately 4200 feet in the Yacht drill hole, UELL. Only those parameters needed by the code are given.

The initial density, $\rho_0 = 2.66$, is an average value of T^2 measurements of wet samples taken from a core specimen retrieved from approximately 4213 feet. The media was assumed to contain 10% H_2O by weight as no measurements were made but the samples were described as wet. No measurements of the bulking factor, Mu_0 , were available for the Yacht shale so the value of -0.15 for the Lewis shale at the Gasbuggy site was used. For this problem, it was felt that the constant Poisson's ratio option in the code was a better representation of the loading path than the constant rigidity modulus option. However, Poisson's ratio as determined from uniaxial strain data shows a definite trend to higher values at higher mean pressures as illustrated in Figure 1. Due to this trend it was decided to run three problems each with a different Poisson's ratio. The values selected were 0.21, 0.31, and 0.35 as it is believed that the initial slope in Figure 1 is more representative of the strain rates that would be encountered during the actual explosion than is the rest of the data.

The pressure-volume data used in the code calculations consist of L^3 measurements up to 40 kbars and Hugoniot data up to 3 megabars used previously by Terhune for Lewis shale. The L^3 P-V data for the Yacht shale and for

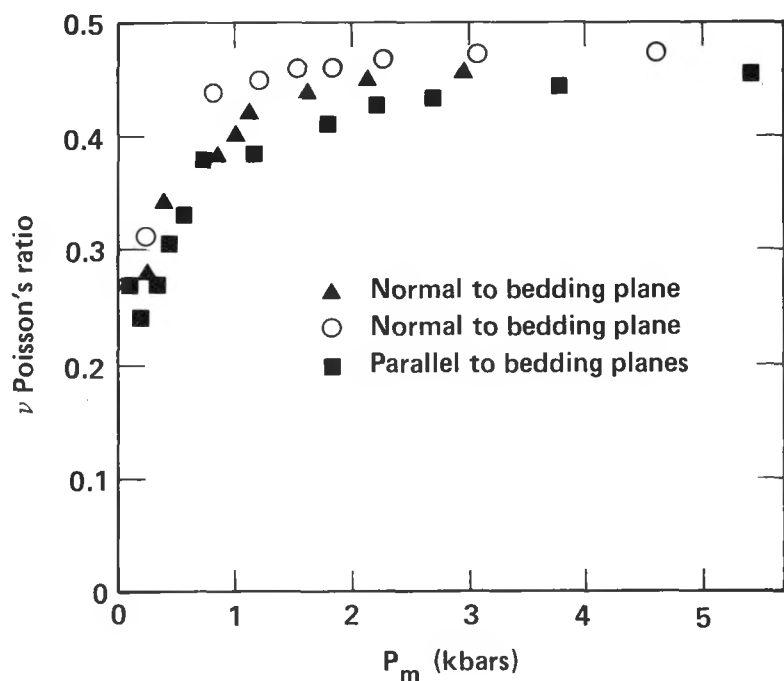


Figure A-1. Poisson's ratio vs mean pressure as determined from uniaxial test data.

Lewis shale are tabulated below. The values chosen arbitrarily to make a smooth curve for Yacht are denoted with an asterisk.

Table A-I. P-V Data.

Yacht Shale		Lewis Shale	
Pressure (kbar)	Mn = $(V_0/V) - 1$	Pressure (kbar)	Mn = $(V_0/V) - 1$
1.5	0.0101*	1	0.00715
3.3	0.0204*	4	0.02145
5.6	0.0309*	8	0.03842
8.3	0.0417*	12	0.05374
11.3	0.0526*	20	0.08108
14.8	0.0638*	28	0.1038*
18.8	0.0753	40	0.1325*
24.1	0.0870	60	0.1798*
30.6	0.989	100	0.2541*
		240	0.5119*
		300	0.6008*
		400	0.7079*
		600	0.8*
		800	0.88*
		1000	0.935*
		1400	1.0*
		2000	1.065*
		3000	1.16*

The compressibilities of the two shales are compared in Figure 2. It can be seen from this Figure that the two are similar at low pressures, thus lending credibility to the use of the Lewis shale data for higher pressures.

Triaxial compression tests were made by both R. Schock of this laboratory and Terra-Tek to determine the failure envelope. Tests were made normal to, parallel to, and at 45° to the bedding planes of the sample and the results are plotted on Figure 3. As can be seen from the figure there exists considerable scatter in the data, so that the failure envelope chosen for input to the code represents at best the average failure behavior of the shale.

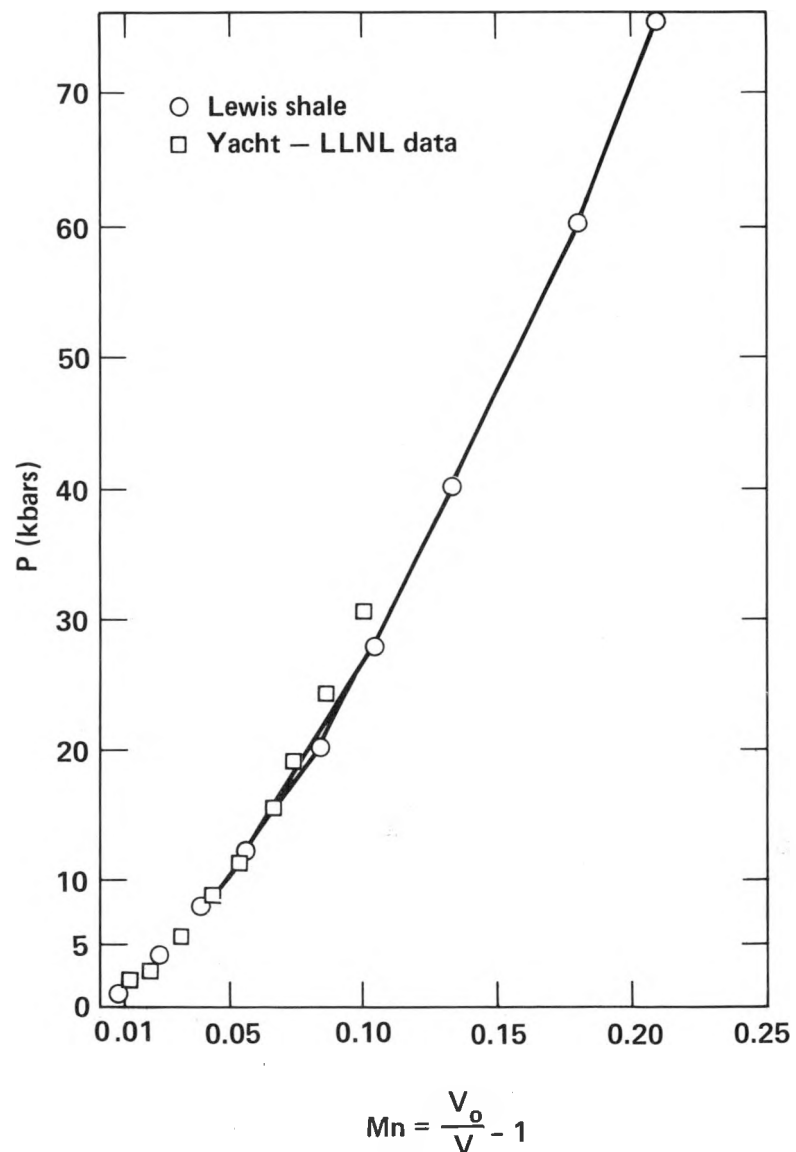


Figure A-2. Compressibility of Yacht and Lewis Shale.

Results of Calculations

Peak values of particle displacement, velocity, acceleration, pressure, and radial stress are given as functions of range in Figures 4-8. All values except those for acceleration are direct code output. The peak acceleration values are estimates made from the particle velocity plots. Each of Figures 4-8 contains the results for the six cases listed below in Table II.

Table A-II. Problems Run on SOC.

ROCK	EXPLOSIVE & DEPTH	R _C	R _f
Wagon Wheel Shale	100 kt	26 m	134 m
Yacht Shale, $v = 0.27$	30 kt @ 4000'	25 m	179 m
$v = 0.31$	30 kt @ 4000'	26 m	174 m
$v = 0.35$	30 kt @ 4000'	27 m	175 m
$v = 0.31$	30 kt @ 2000'	26 m	230 m
$v = 0.31$	100 kt @ 4000'	38 m	290 m

For each parameter holding yield constant, the case of Poisson's ratio of 0.35 has highest values. To compare the effect of yield and depth on the results of the calculations, Poisson's ratio was held constant at 0.31. For reference the calculated values for the Wagon Wheel experiment have also been plotted on these Figures. For every parameter except the peak particle displacement the calculated values for Wagon Wheel exceed those for Yacht.

Figures 9 through 12 show the locations of the shock front, the extent of fracture, and the cavity radius as functions of time. It is seen that the cavity radius for all but 100 kt in Yacht rock are about the same whereas the extent of fracture for every case of Yacht rock exceeds that of Wagon Wheel, see Table II.

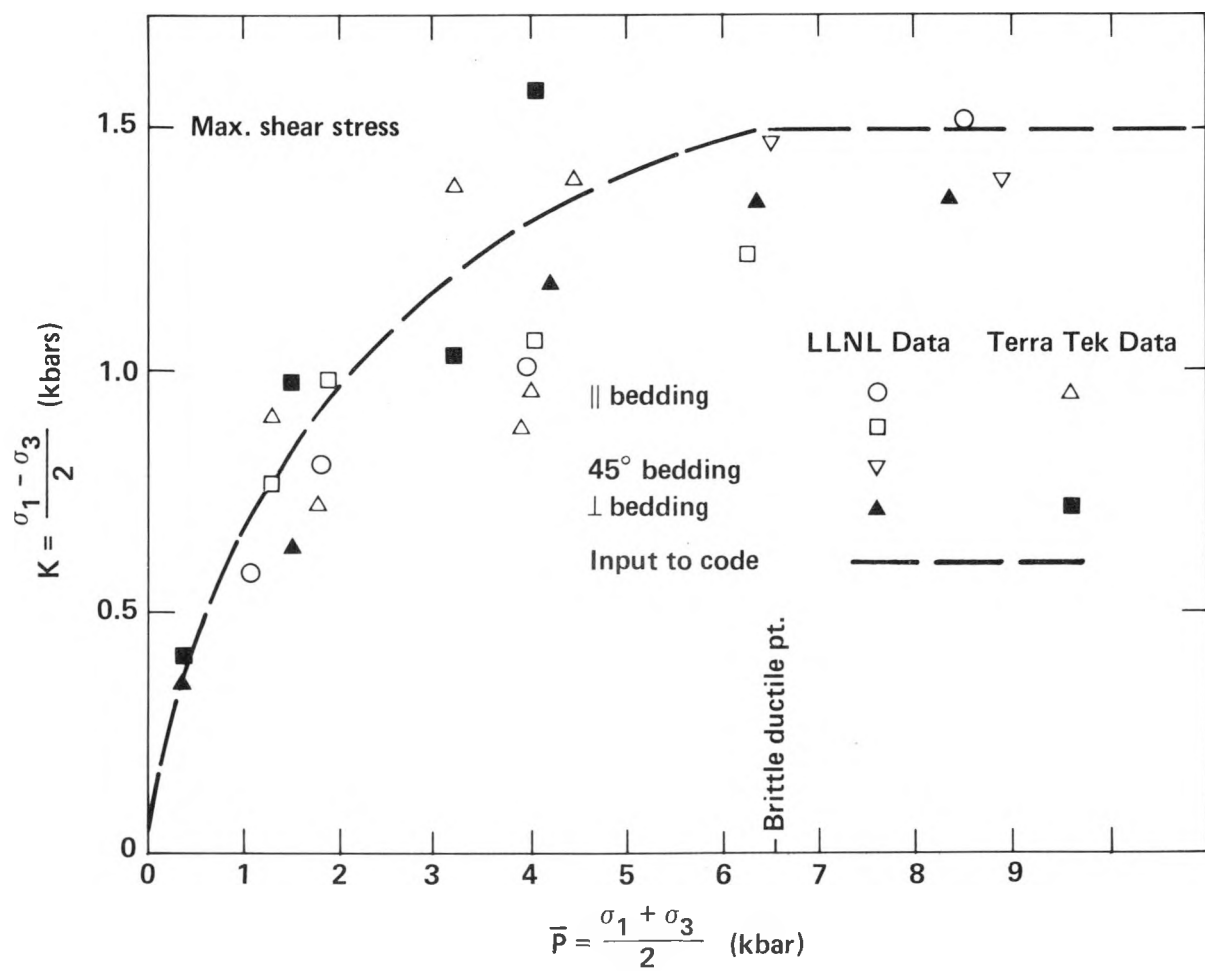


Figure A-3. Triaxial compression test data.

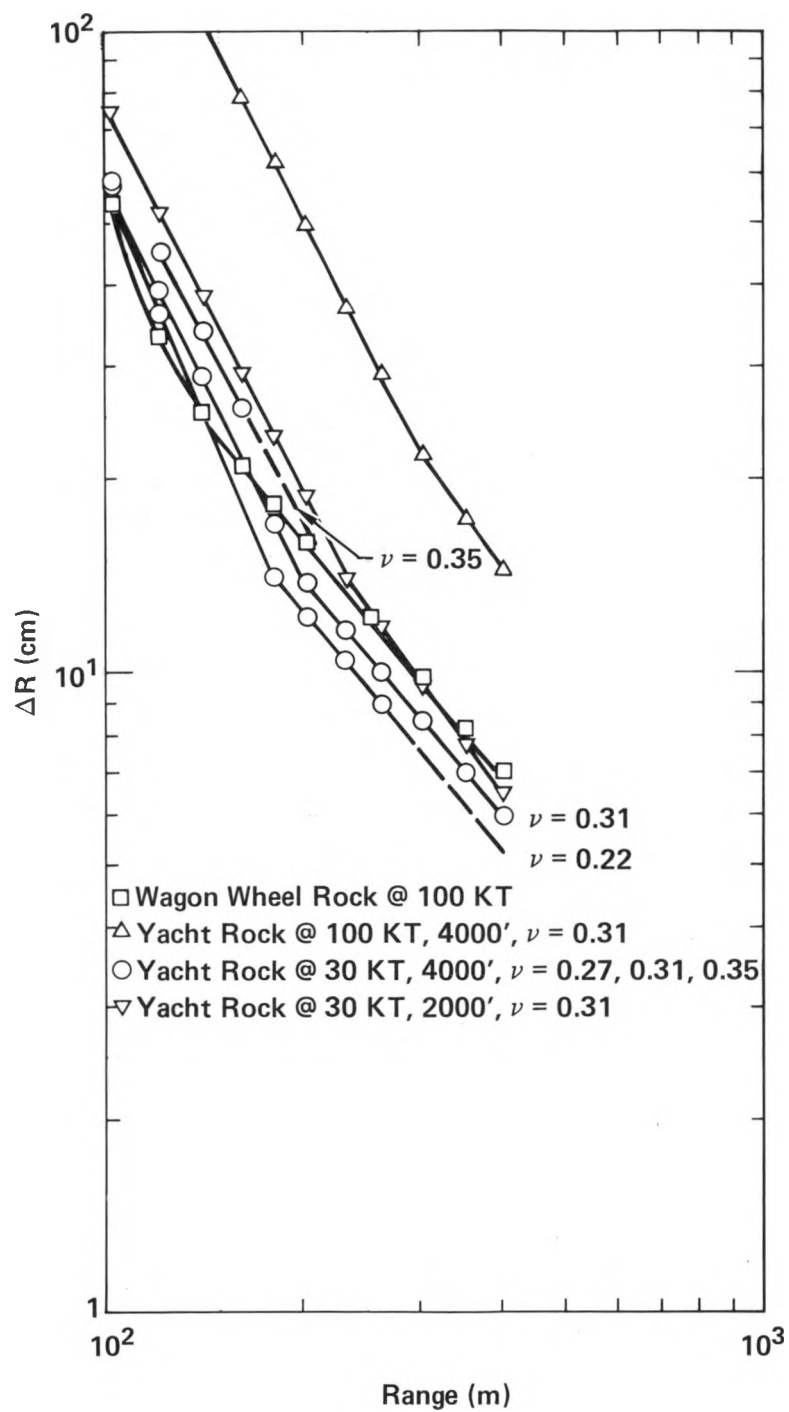


Figure A-4. Peak displacement vs range.

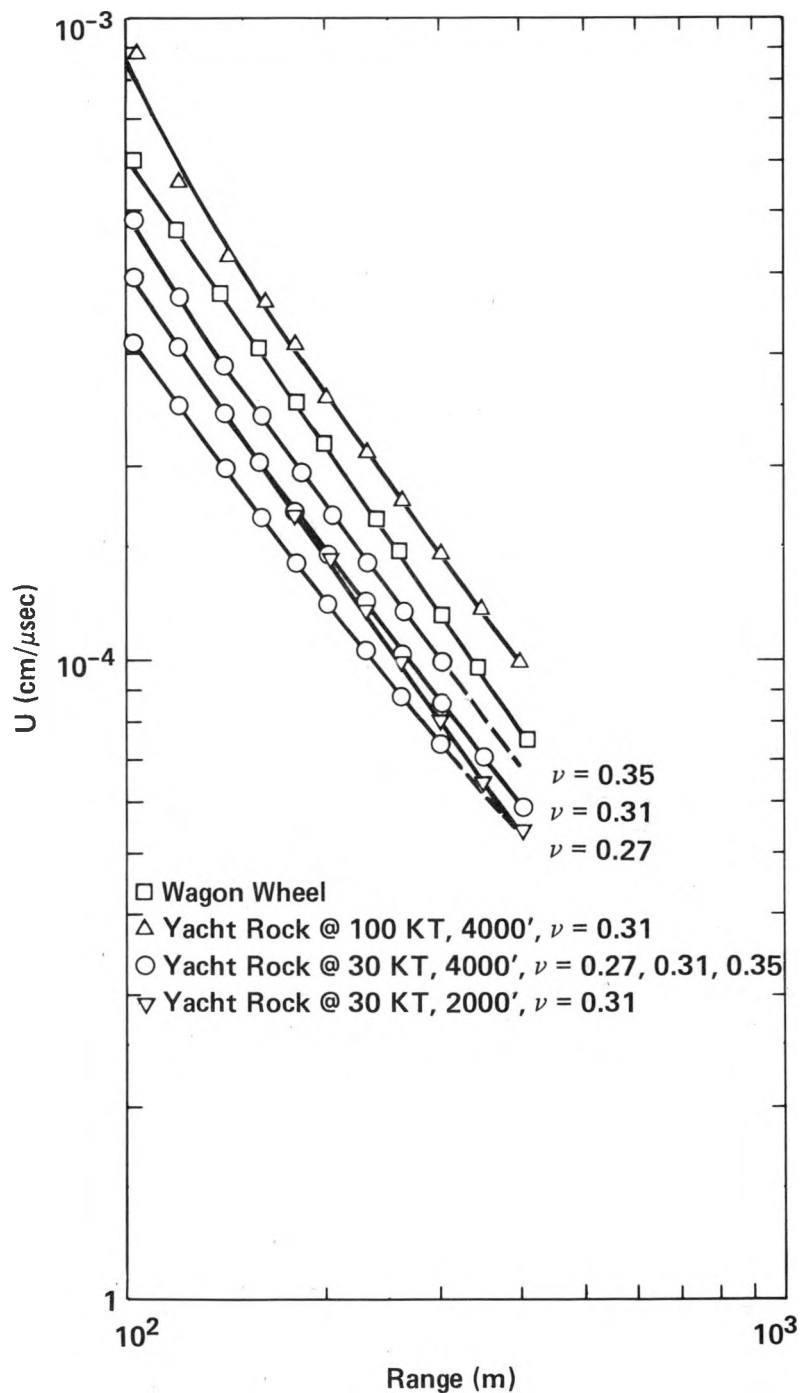


Figure A-5. Peak velocity vs range.

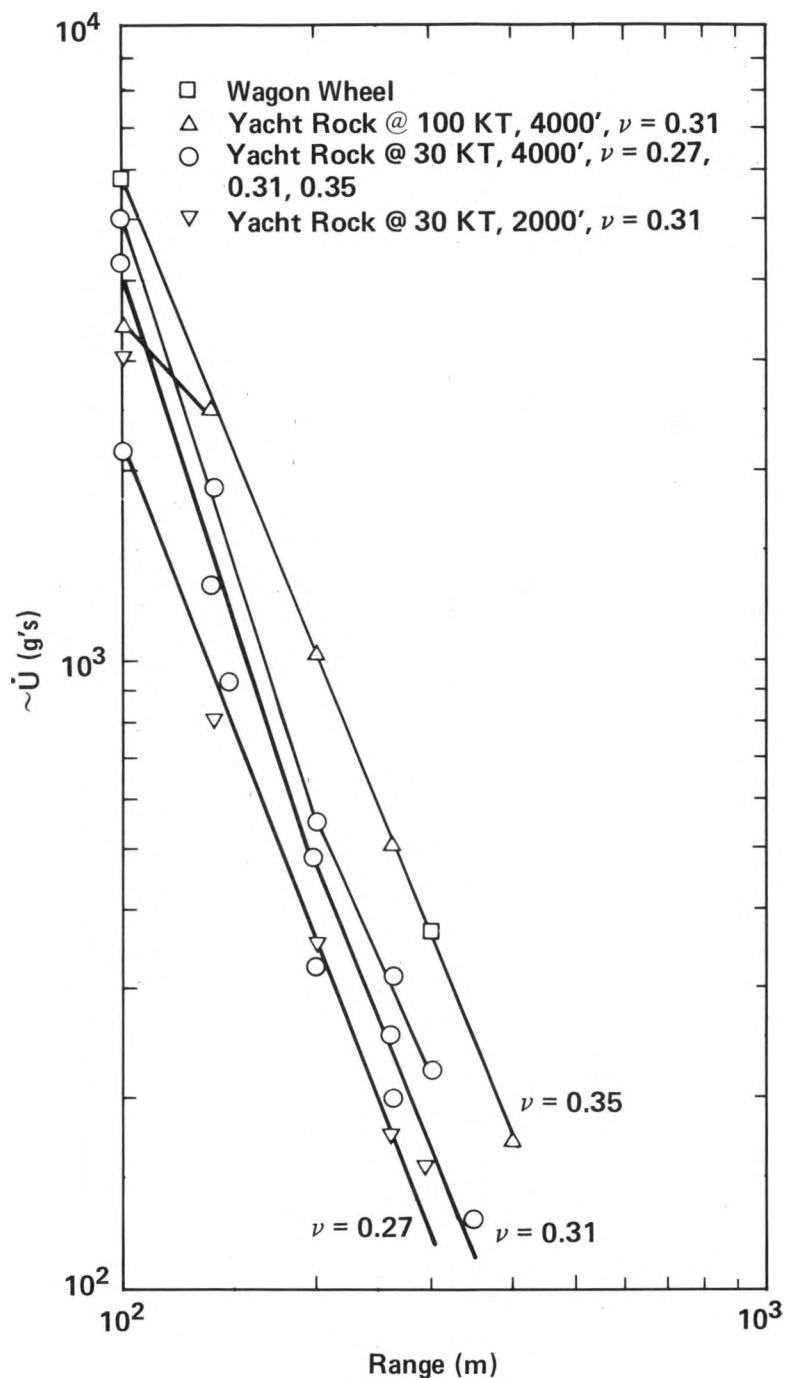


Figure A-6. Maximum acceleration vs range.

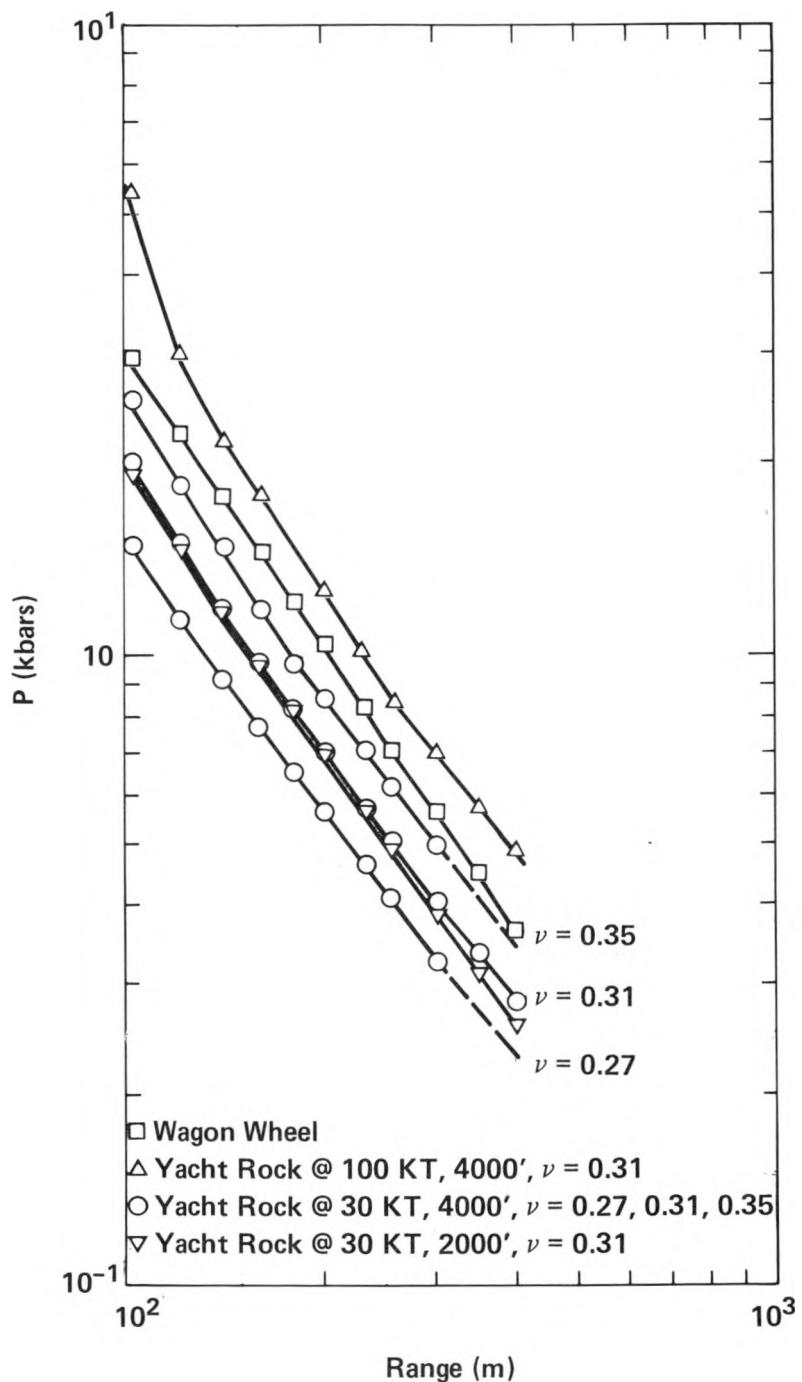


Figure A-7. Peak pressure vs range.

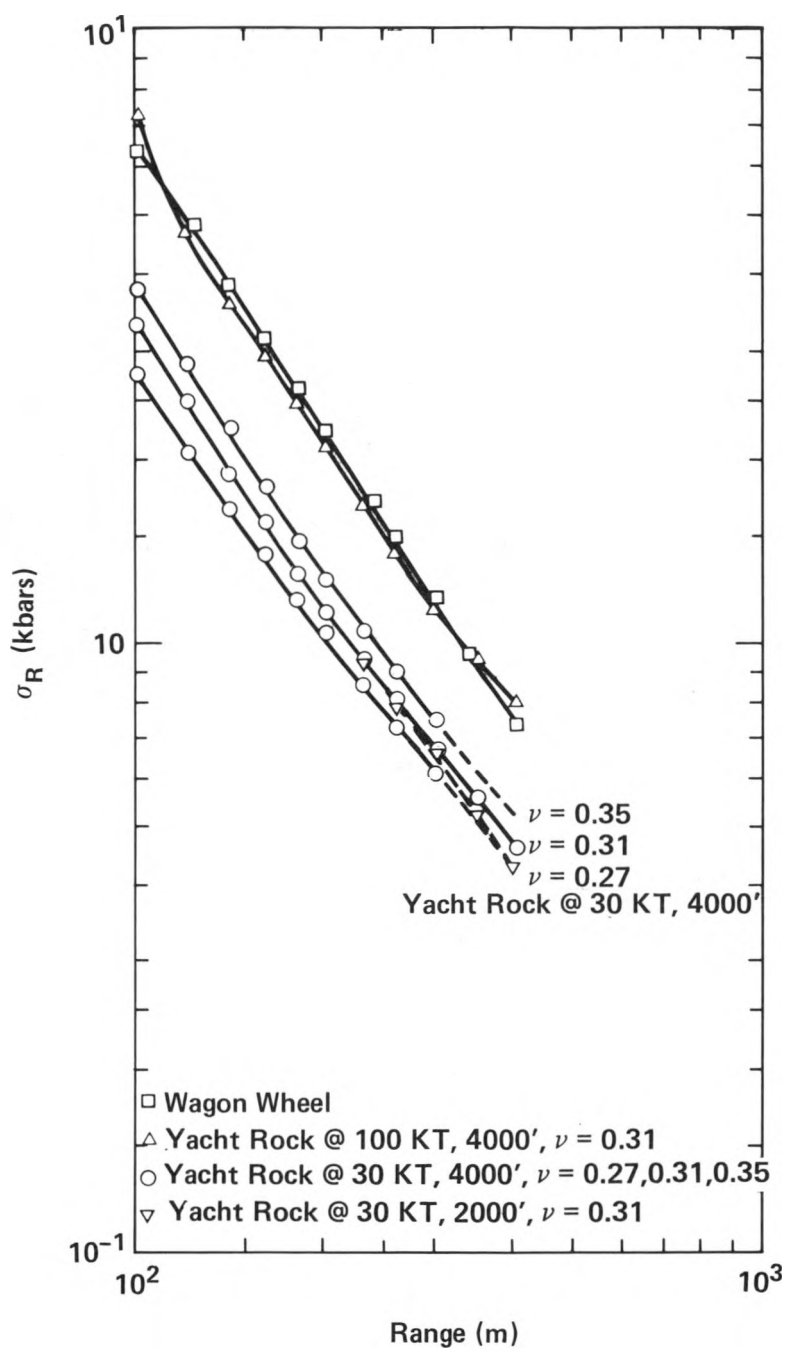


Figure A-8. Peak radial stress vs range.

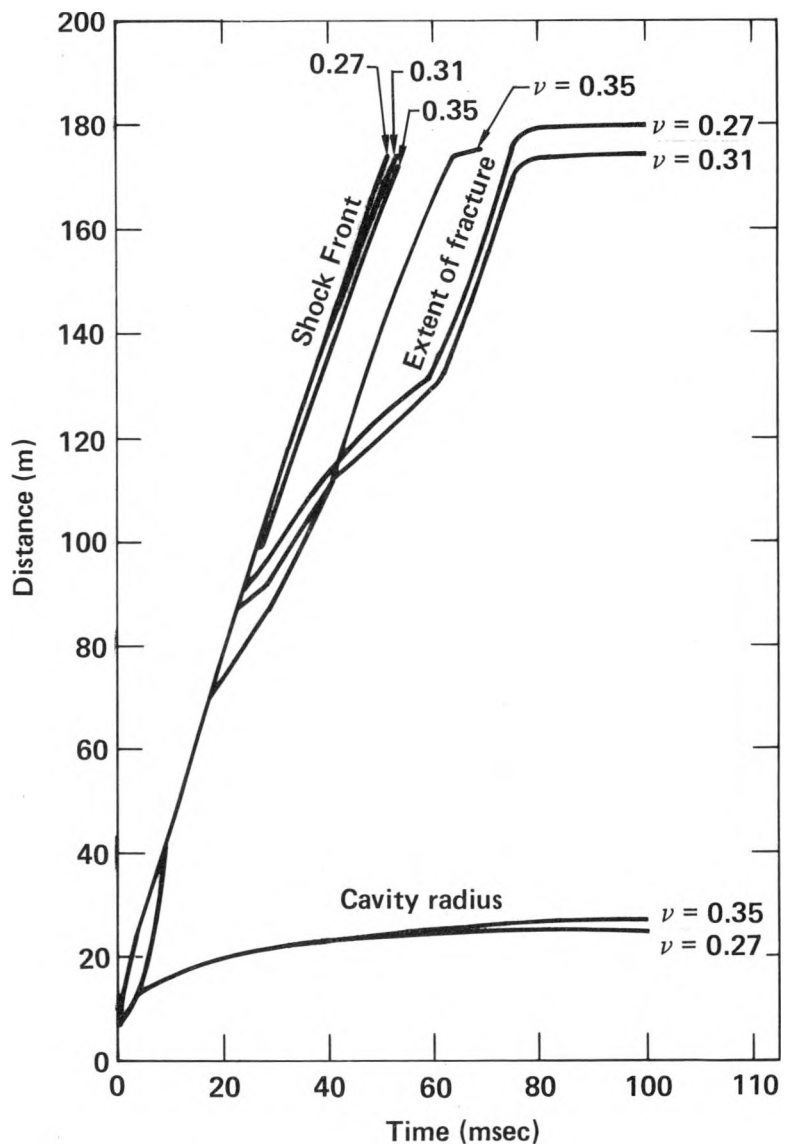


Figure A-9. Arrival times in Yacht Rock @ 30 KT,
4000 ft.

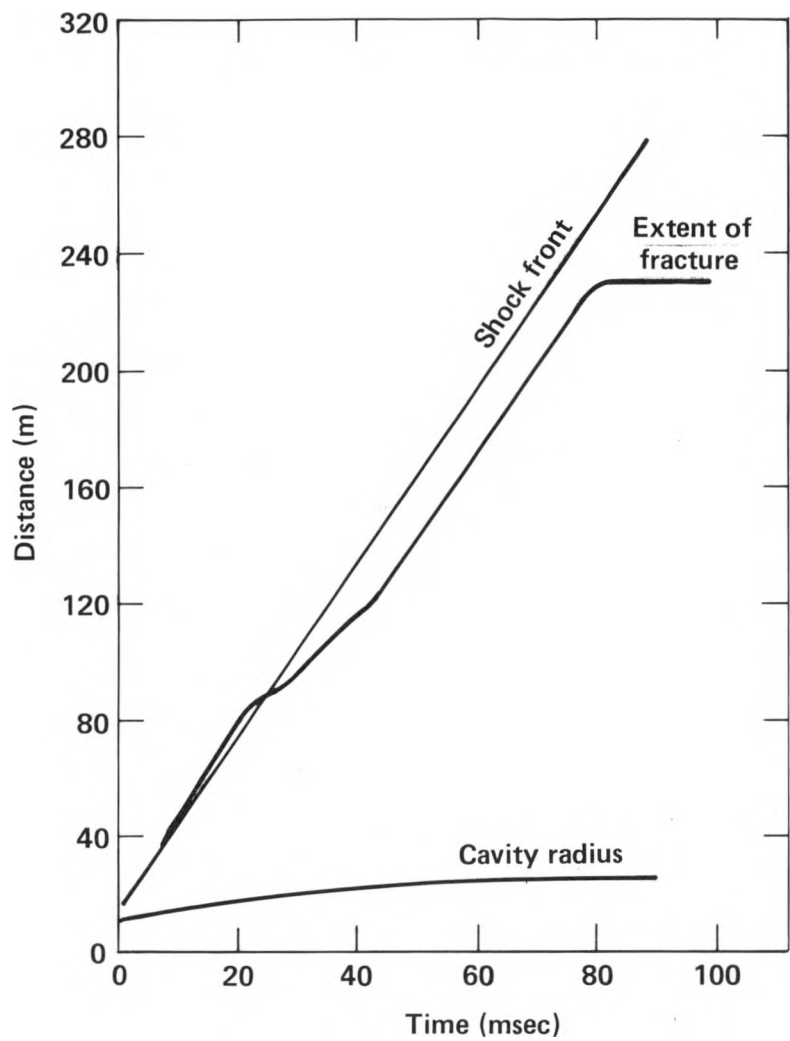


Figure A-10. Arrival times in Yacht Rock @ 30 KT,
2000 ft.

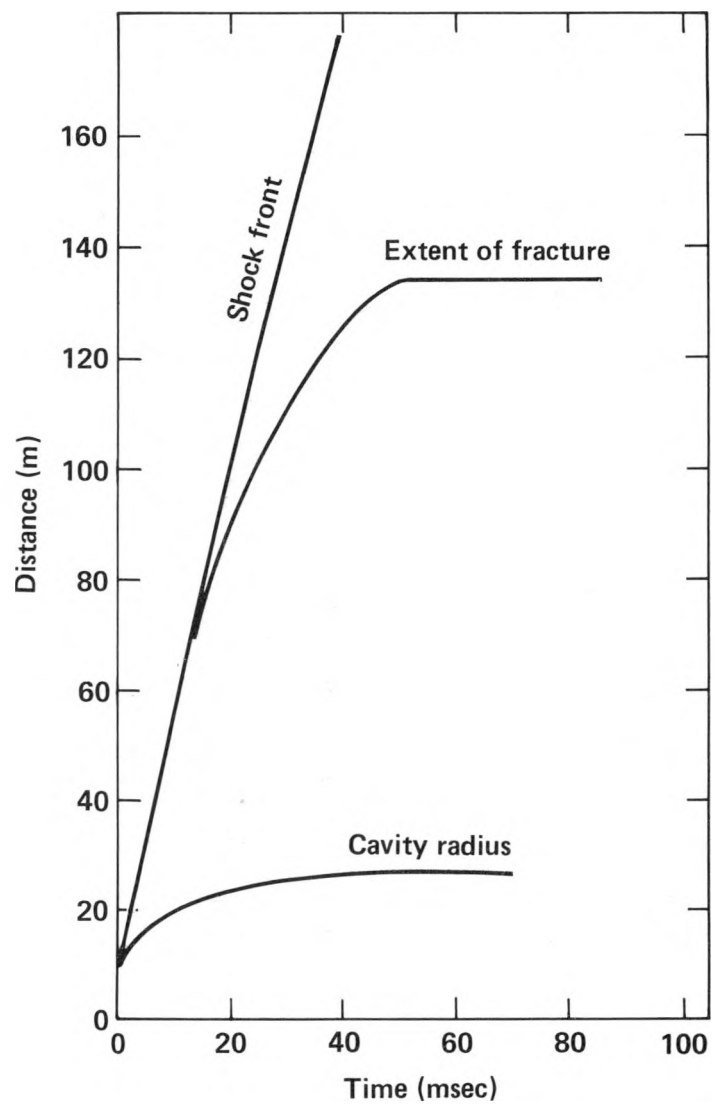


Figure A-11. Arrival time for Wagon Wheel.

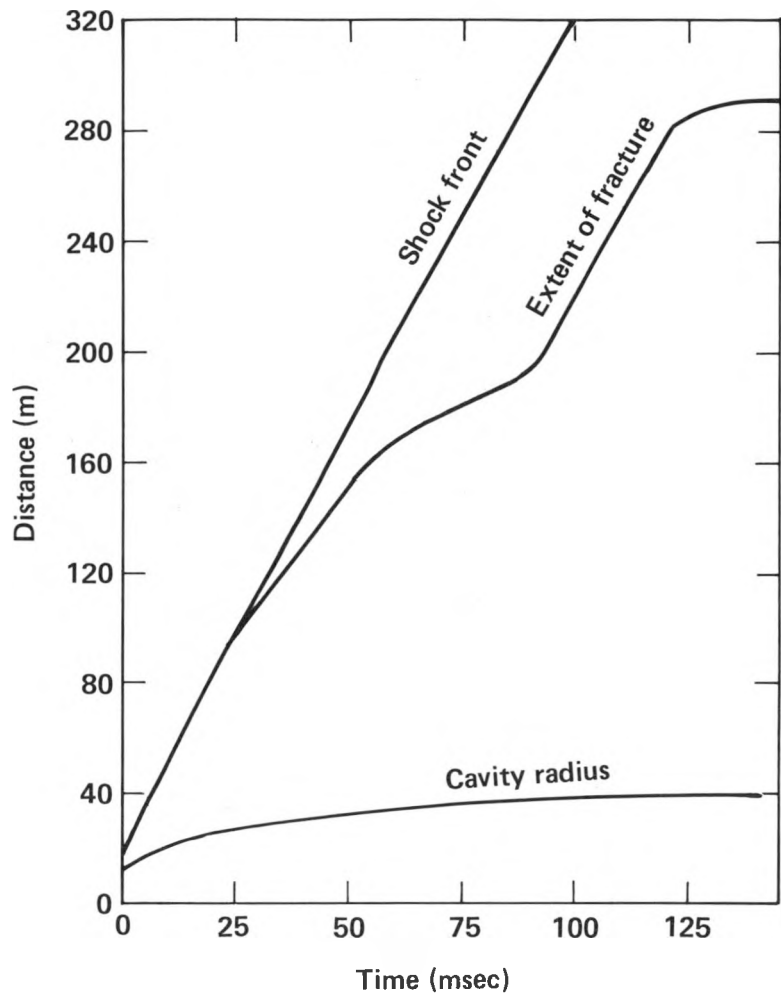


Figure A-12. Arrival time in Yacht Rock @ 100 KT,
4000 ft.

APPENDIX B

Table B-1. List of Holes Drilled Into the Eleana Formation.

Location In The NTS	Hole Number	Depth To Eleana (m)	Total Depth (m)
Yucca Flat	UE1a	274.0	292.0
Area 1	UE1b	231.0	382.0
	UE1r	514.0	519.0
	UE1f	171.0	214.0
	UE1L	80.0	1627.0
Yucca Flat	UE2a-1	196.9	228.5
Area 2	UE2b	313.0	326.3
	UE2dy	169.2	173.0
Yucca Flat	T.W.-D	164.6	181.1
Area 4	UE4ab	242.9	246.3
	UE4af	130.5	138.4
Yucca Flat	U8a4	112.8	178.8
Area 8	U8a5	118.0	177.9
	U8all	147.8	180.7
Areas 16,17	UE1bb	96.6	110.0
Syncline Ridge	UE1bc	36.6	43.9
Area	UE1bd	452.9	914.4
	UE1bf	24.1	451.1
	UE17a	166.4	370.0
	UE17b	67.1	78.2
	UE17d	-	-
	UE17e	0	914.4
Area 25	UE25a-3	0	771.2
Calico Hills			

References

1. McKague, H. L., Summary of Measured Medium Properties of Paleozoic Rocks at the DOE Nevada Test Site, Lawrence Livermore National Laboratory, Livermore, CA, UCRL-52884 (1980).
2. Sinnock, S., Geology of the Nevada Test Site and Nearby Areas, Southern Nevada, Sandia National Laboratory, SAND82-2207 (1982), 60 pp.
3. Connolly, J. R., Woodward, L. A., Emanuel, K. M., and Keil, K., Field Examination of Shale and Argillite in Northern Nye County, Nevada, Sandia National Laboratory, SAND81-7154 (1981), 48 pp.
4. Simpson, H. E., Weir, J. W., and Woodward, L. A., Inventory of Clay-Rich Bedrock and Metamorphic Derivatives in Eastern Nevada, Excluding the Nevada Test Site, USGS Open File 79-760 (1979), 136 pp.
5. Ekren, E. B., Anderson, R. E., Rogers, C. L., and Noble, D. C., Geology of Northern Nellis Air Force Base Bombing and Gunnery Range, Nye County, Nevada, USGS Prof. Paper 651 (1971), 91pp.
6. McKay, E. J., and Williams, W. P., Geology of the Jackass Flats Quadrangle, Nye County Nevada, USGS Geological Quad. Map GQ-368 (1964).
7. McKeown, F. A., Healey, D. L. and Miller, C. H., Geologic Map of the Yucca Lake Quadrangle, Nye County, Nevada, USGS Geological Quad. Map GQ-1327 (1976).
8. Orkild, P. P., Geologic Map of the Mine Mountain Quadrangle, Nye County, Nevada, USGS Geological Quad. Map GQ-746 (1968).
9. Orkild, P. P., Geologic Map of the Tippipah Spring Quadrangle, Nye County, Nevada, USGS Geological Quad. Map GQ-213 (1963).
10. Gibbons, A. B., Hinrichs, E. N., Hansen, W. R., and Lemke, R. W., Geology of the Rainier Mesa Quadrangle, USGS Geological Quad. Map GQ-215 (1963).
11. McArthur, R. D., The Subsurface Geology of the Lawrence Livermore Laboratory Portion of Area 4 at the Nevada Test Site, Lawrence Livermore National Laboratory, Livermore, CA, UCRL-52061 (1976), 31 pp.
12. Hoover, D. L., and Morrison, J. N., Geology of the Syncline Ridge Area Related to Nuclear Waste Disposal, Nevada Test Site, Nye County, Nevada, USGS Open File 80-942 (1980), 69 pp.
13. Barnes, H., Hinricks, E. N., McKeown, F. A., and Orkild, P. P., U. S. Geological Survey Investigations of Yucca Flat, Nevada Test Site, Part A - Geology of the Yucca Flat Area, Technical Letter NTS-45 (1963).
14. Poole, F. G., Houser, F. N., and Orkild, P. P., Eleana Formation of the Nevada Test Site and Vicinity, Nye County Nevada, in Short Papers in Geologic and Hydrologic Sciences, USGS Prof. Paper 424-D (1961), pp. D104-D111.

15. Johnson, M. S., and Hibbard, D. E., Geology of the Atomic Energy Commission Nevada Proving Grounds Area, Nevada, Geologic Survey Bulletin 1021-K (1957), pp. 333-384.
16. Poole, F. G., and Sandberg, L.A., "Mississippian Paleogeography and Tectonics of the Western United States," in Paleozoic Paleogeography of the Western United States, Pacific Coast Paleogeography Symposium 1, J. H. Stewart and others, Eds., Pacific Section, Soc. Econ. Paleontologists and Mineralogists (1977), pp. 67-86.
17. Hodson, J. N., and Hoover, D. L., Geology of the Uel7e Drill Hole, Area 17 NTS, USGS Report 1543-2 (1979), 36 pp.
18. Bates, R. L., and Jackson, J. A., Eds., Glossary of Geology, Second Edition, American Geological Institute, Falls Church, VA (1980), 749 pp.
19. Simonson, E. R., Green, S. J., Butters, S. W., Rogers, L. A., and Jones, A. H., Stress-strain and Failure Response of the Yacht Site Shale, Terra-Tek, Inc., Tech. Report TR72-26 (1972), 45 pp.
20. Hill, J. H., "Chemical Analysis of Argillite," memo to D. Emerson, LLL internal memo (1970).
21. Blackmon, P. D., USGS Laboratory Report DEG-251 (1974).
22. Seismograph Service Corp., Report on a Vibroseis Seismic Survey Conducted in Nye County, Nevada, Yacht Prospect (1972), 25 pp.
23. Carroll, R. D., "Yacht Electrical Sounding Survey," Letter to D. O. Emerson, UOPKL 72-13 (Mar. 7, 1972).
24. Carroll, R. D., letter to D. O. Emerson (Jul. 7, 1972).
25. Emerick, W. L., Exploratory Drill Holes Uela, Uelb, and Uelc, Yucca Flat, Nevada Test Site, USGS Technical Letter Yucca-54 (1964), 15 pp.
26. Emerick, W. L., Gard, L. M., and Williams, W. P., Exploratory Drill Holes Ueld, Uele, Uelf, and Uelg, Area 1, Yucca Flat, Nevada Test Site, USGS Technical Letter Yucca-55 (1964), 16 pp.
27. Denny, M. D., "SOC Calculations of the Dynamic Behavior of Yacht Rock," LLL internal memo UOPKL 72-60 (Dec. 5, 1972).
28. Bernreuter, D. L., and Jackson, E. C., Estimates of Ground Motion from the Proposed Yacht Event and its Effects on Key Facilities, Engineering Note ENN 72-71, Lawrence Livermore National Laboratory, Livermore, CA, (Apr. 13, 1972), 8 pp.
29. Maldonado, F., Muller, D. C., and Morrison, J. N., Preliminary Geologic and Geophysical Data of the Ue25a-3 Exploratory Drill Hole, Nevada Test Site, Nevada, USGS Report 1543-6 (1979), 43 pp.
30. Wier, J. E., and Hudson, J. N., Geohydrology of Hole Uel7a, Syncline Ridge Area, Nevada Test Site, USGS Report-1543-4 (1979), 18 pp.

31. Dinwiddie, G. A., and Wier, J. E., Jr., Summary of Hydraulic Tests and Hydrologic Data for Holes Uel6d and Uel6f, Syncline Ridge Area, Nevada Test Site, USGS Report-1543-3 (1979), 25 pp.
32. Hodson, J. N. and Hoover, D. L., Geology and Lithologic Logs for Drill Hole Uel7a, Nevada Test Site, USGS Report-1543-1 (1978), 17 pp.
33. Anderson, L. A., Bisdorf, R. J., and Schoenthaler, D. R., Resistivity Sounding Investigation by the Schlumberger Method in the Syncline Ridge Area, Nevada Test Site, Nevada, USGS Open File Report 80-466 (1980), 64 pp.
34. Hoover, D. B., Hanna, W. F., Anderson, L. A., Flanigan, V. J., and Pankratz, L. W., Geophysical Studies of the Syncline Ridge Area, Nevada Test Site, Nye County, Nevada, USGS Open File Report 82-145 (1982), 67 pp.
35. Lappin, A. R., Thomas, R. K., McVey, D. F., Eleana Near-Surface Heater Experiment Final Report, Sandia National Laboratory Report SAND80-2137 (1981), 50 pp.
36. Fernald, A. T., Byers, F. M., and Ohl, J. P., Lithologic Logs and Stratigraphic Units of Drill Holes and Mine Shafts in Areas 1 and 6, Nevada Test Site, USGS Report 474-206 (1975), 62 pp.
37. Jenkins, E. C., "Geology of the Yacht Site Area," Letter to D. O. Emerson (May 24, 1973).
38. Turner, P., "Chemical Analysis of Argillite," internal LRL memo to D. O. Emerson (1971).
39. Turner, P., "Porosity-Density Measurements-UelL," memo to D. O. Emerson, UOPKB 72-84 (Oct. 31, 1972).
40. Jones, L. E. A., and Wang, H. F., "Ultrasonic Velocities in Cretaceous Shales from the Williston Basin," Geophysics 46 (3), 288 (1981).
41. Harri, John, "Yacht UelL Downhole Temperature," Letter to D. O. Emerson, UOPKL 72-57 (Oct. 16, 1972).
42. Barnes, H., and Poole, F. G., Regional Thrust-Fault System in Nevada Test Site and Vicinity, E. B. Eckel, Ed., GSA Memoir 110 (1968), pp. 233-246.
43. Butler, R. W. H., "The Terminology of Structures in Thrust Belts," J. Struct. Geology 4, 239-245 (1982).
44. Dahlstrom, C. D. A., "Balanced Cross Sections," Canadian J. of Earth Sciences 6, 743-757 (1969).
45. Elliott, D., and Johnson, M. R. W., "Structural Evolution in the Northern Part of the Moine Thrust Belt, NW Scotland," Trans. Royal Soc., Edinburgh, Earth Sciences 71, 69-96 (1980).
46. Donath, F. A., and Parker, R. B., "Folds and Folding," Geol. Soc. Amer. Bull. 75, 45-62 (1964).

47. Yeats, R. S., "Large-scale Quaternary Detachments in Ventura Basin, Southern California," J. Geophys. Res. 88 (81) 569-583 (1983).
48. Brock, W. G., and Engelder, T., "Deformation Associated with the Movement of the Muddy Mountain Overthrust in the Buffington Window, Southeastern Nevada," G. S. A. Bull. 88, 1667-1677 (1977).
49. Guth, P. L., "Tertiary Extension North of the Las Vegas Valley Shear Zone, Sheep and Desert Ranges, Clark County, Nevada," G.S.A. Bull., Part I 92, 763-771 (1981).
50. Burchfiel, B. C., Wernicke, B., Willemin, J. H., Axen, G. J., and Cameron, C. S., "A New Type of Decollement Thrusting," Nature 300, 513-515 (1982).
51. Johnson, M. R. W., "The Erosion Factor in the Emplacement of the Keystone Thrust Sheet (Southeast Nevada) Across a Land Surface," Geol. Mag. 118 (5) 501-507 (1981).
52. Robinson, G. D., USGS, Menlo Park, CA, personal communication (1983).